NASA CONTRACTOR
REPORT

NASA CR-61242

September 23, 1968

NASA CR-61242

GPO PRICE $ _____

CSFTI PRICE(S) $ _____

Hard copy (HC) 3.00

Microfiche (MF) .65

ff 653 July 65

WIND TOWER INFLUENCE STUDY

(For NASA's 150-Meter Meteorological Tower at Kennedy Space Center, Florida)

Prepared under Contract No. NAS 8-5608 by
J. W. Hathorn

THE BOEING COMPANY

For

NASA-GEORGE C. MARSHALL SPACE FLIGHT CENTER
Marshall Space Flight Center, Alabama

September 23, 1968 NASA CR-61242

WIND TOWER INFLUENCE STUDY
(For NASA's 150-Meter Meteorological Tower at Kennedy Space Center, Florida)

By

J. W. Hathorn

Prepared under Contract No. NAS 8-5608 by

THE BOEING COMPANY

For

Aero-Astrodynamics Laboratory

NASA-GEORGE C. MARSHALL SPACE FLIGHT CENTER

REVISIONS

REV. SYM	DESCRIPTION	DATE	APPROVED

ABSTRACT AND LIST OF KEY WORDS

The primary function of NASA's 150-meter meteorological tower facility located in the vicinity of Launch Complex 39 at the Kennedy Space Center, Florida, is to acquire lower atmosphere data for use in research and engineering studies that assist in the development of NASA's space vehicle environmental criteria. Because the environmental criteria are based upon studies that utilize tower data, the data must be as free as possible from distorting influences. The tower influence upon wind measurements is the primary concern of this study since it is necessary to establish correction factors to adjust the wind measurements to represent ambient mean winds if this distorting influence is significant.

An experimental study was designed after making a thorough literature search. This study provided data used to judge whether or not NASA's 150-meter meteorological tower significantly influenced the wind measurements and to establish correction factors to these wind measurements if required. The correction factors were computed by determining the ratios and deviations between the measured and reference mean wind speeds and directions, respectively. Prior to determining these correction factors, two investigations were performed to study whether or not: (1) the tower influence field is bilaterally symmetrical about the structural axis of symmetry, and (2) the influence fields are the same for all levels of the tower.

The maximum influence on the wind speed was found to occur when the wind flow was through the tower; ratios of 0.73 were noted. A ratio of 1.03 was computed for northwest winds normal to the booms and a ratio of 0.94 was obtained at the windward sensor for northeast winds parallel to the booms. The maximum direction deviation (-9 degrees) occurred when the wind was from the east-southeast and the minimum deviations (±2 degrees) occurred when the winds were from the north quadrant. Deviations in the wake were not large; however, data were erratic due to the perturbed flow.

In a supporting theoretical study, the stream function was computed about a solid triangular tower (with and without catwalk) using a numerical technique to solve Laplace's equation ($\nabla^2\psi=0$). The maximum speed ratio at the boom tip position with the wind normal to the boom was found to be 1.035 for the solid triangular tower without catwalk and was found to be 1.045 for the solid triangular tower with catwalk.

Meteorological Tower Influence
Wind Profile Measurement
Wind Tower Influence
Wind Velocity Measurement

CONTENTS

ILLUSTRATIONS

ILLUSTRATIONS (Continued)

APPENDIX ILLUSTRATIONS

TABLES

REFERENCES

1. "NASA's 150-Meter Meteorological Tower Located at Kennedy Space Center, Florida", J. W. Kaufman and L. F. Keene, NASA TM X-53699, Revised January 29, 1968.

2. "Errors in Measurements of Wind Speed and Direction Made with Tower - or Stack - Mounted Instruments", G. C. Gill, L. E. Olsson, M. Suda, University of Michigan, ORA Project 06973, June, 1966.

3. "Results of a Wind Tunnel Program to Investigate the Interference or Shadowing Effects of a Meteorological Tower", R. A. Meyer, H. B. Reese and J. R. Ziler, Chrysler TN-AE-65-98, New Orleans, Louisiana, July 8, 1965.

4. "Meteorological-Tower Induced Wind-Field Perturbations", G. Hsi and J. E. Cermak, Colorado State University, May, 1966 (DDC No. AD-633-353).

5. "What Are We Measuring on the Top of a Tower?", M. Sanuki and N. Tsuda, Papers in Meteorology and Geophysics VIII, Tokyo, Japan, pp. 99-101, 1957.

6. "Wind Tunnel Tests on Models of Kennedy Space Center Structures", J. Vellozzi, Ammann & Whitney Consulting Engineers, New York, New York, Contract No. DA-08-176-ENG (NASA)-341, September, 1967.

7. "Errors in Wind Measurements Associated with Tower-Mounted Anemometers", H. Moses and H. G. Daubek, Bulletin American Meteorological Society, Vol. 42, No. 3, March, 1961, pp. 190-194.

8. "Tower-Induced Errors in Wind Profile Measurements", W. F. Dabberdt, Journal of Applied Meteorology, Vol. 7, No. 3, June, 1968, pp. 359-366.

9. "Disturbance of Airflow Around Argus Island Tower Near Bermuda", C. W. Thornthwaite, W. J. Superior, and R. T. Field, Journal of Geophysical Research ,Vol. 70, No. 24, December 15, 1965, pp. 6047-52.

10. "Evaluation of the Effects of the Structure of a 300-Meter Meteorological Mast on the Readings of Wind-Velocity Pickups", E. V. Borovenko, O. A. Volkovitskiy, L. M. Zolotarev, and S. A. Isayeva, Investigation of the 300-Meter Lower Layer of the Atmosphere, (A collection of papers published by the Academy of Sciences of the U.S.S.R.), 1963, pp. 104-115 (DDC No. AD-620-052).

11. "Tower Shadow Effects", J. E. Cermak and J. D. Horn, Journal of Geophysical Research, Vol. 73, No. 6, March 15, 1968, pp. 1869-1876.

12. "Experience with Studying the Wind Field Around a Cylindrical Tower with Balconies", A. A. Dmitriyev, The Soviet 300-Meter Meteorological Tower, March 25, 1964, pp. 162-185, (DDC No. AD-622-236).

REFERENCES (CONTINUED)

13. "Anemometer Reading in the Presence of Nearby Obstacle", M. Sanuki, S. Kimura, and S. Toyama, Papers in Meteorology and Geophysics VI, Tokyo, Japan, 1955, pp. 140-143.

14. "Drag of Circular Cylinders for a Wide Range of Reynolds Numbers and Mach Numbers", E. Forrest, E. Gowen, and E. Perkins, NACA-TN-2960, June, 1953.

15. "Boeing Thermal Analyzer", (Part 1, Engineering Usage Guide), Boeing Document AS 0315, J. C. Almond, August 21, 1964.

16. Theoretical Hydrodynamics, L. M. Milne-Thomson, The Macmillan Company, New York, 1960.

PREFACE

This document has been prepared by the Postflight Trajectories Group to satisfy the technical requirements specified by Data Requirements Description SE-666, Exhibit CC, Contract NAS8-5608, Schedule II, Part II, Section A, Task 8.1.7. The task performed was in support of the Aerospace Environment Division, Atmospheric Dynamics Branch (R-AERO-YE), Marshall Space Flight Center, National Aeronautics and Space Administration, with John W. Kaufman as technical coordinator.

The author wishes to thank J. W. Kaufman and D. W. Camp (Aero-Astrodynamics Laboratory, MSFC/NASA) for their services in coordinating the technical portions of this program; A. L. Jackson (Computation Laboratory, MSFC/NASA) for his services in digitizing the data and computing spectra; L. F. Keene (Data Systems Division, KSC/NASA) for his assistance in coordinating operations at the tower facility; and A. Raasch (Pan American World Airways, KSC) for acquiring the data necessary for the completion of this study. A special acknowledgement is due W. W. Vaughan (Chief, Aerospace Environment Division, MSFC/NASA for his advice throughout this program and for his critique of the final report.

In addition, the author would like to express his gratitude to R. D. McCurdy for his supervision and to R. S. Wheeler for his discussions and advice in the preparation of this report.

SOURCE DATA PAGE

The following listed government-furnished data has been used in preparation of this document release:

Exhibit FF Line Item Number		DATE OF ISSUE
AERO 24b	Meteorological Environmental Data - 249 Magnetic Tapes Containing Data Records from NASA's 150-Meter Meteorological Tower Facility	From 4/11/67 Through 6/28/68

SECTION 1

INTRODUCTION

1.0 BACKGROUND

When a tower is used to support wind sensors at several heights, the tower itself may alter the free-stream flow of the wind and thereby influence the measurements acquired by the sensors. The amount of influence is a function of (1) the proximity of the sensors to the tower, (2) the speed and direction of the wind with respect to the sensors and the tower, and (3) the structural design of the tower (secondary members, catwalks, booms, cables, etc.). To translate the wind velocity measurements into free-stream velocities with a high level of confidence, quantitative knowledge of the influence is required.

NASA's 150-meter meteorological tower (Reference 1), located in the vicinity of Launch Complex 39 at the Kennedy Space Center, Florida, is a steel lattice tower that supports wind sensors and other meteorological instruments at several heights above the ground (Figure 1-1). The horizontal cross-section of the tower (Figure 1-2) is a 2.45 meter (8 foot) equilateral triangle, and the wind sensors are attached near the tips of 3.66 meter (12 foot) booms that extend northeast and southwest of the tower. A wind direction selector is employed to determine which sensor (northeast or southwest) is windward of the tower and, in normal operations, to select it for monitoring the wind (Reference 1). This dual boom orientation makes the tower structurally symmetrical about a northwest-southeast line. The primary function of this tower facility is to acquire lower atmosphere data for use in research and engineering studies to develop NASA's space vehicle environmental criteria.

1.1 DEFINITION OF PROBLEM

The tower influence problem, discussed in this document, is stated in the following manner:

> To determine whether or not NASA's 150-meter meteorological tower located at Kennedy Space Center significantly influences the winds as measured by the sensors mounted upon it, and if so, to provide the means to uniquely correct the measured wind speeds and directions to approximate the free-stream wind.

One method of solving the stated problem is to determine a set of correction factors that can be applied to the measured mean wind speed and direction so that close approximations of the mean speed and direction of the free-stream wind can be obtained. These correction factors can then be used to study quantitatively the amount of tower influence and to obtain any necessary speed and direction corrections. The desired correction factors can be determined either experimentally or theoretically. Experimentally, measured winds are compared to winds obtained from a "reference" sensor in

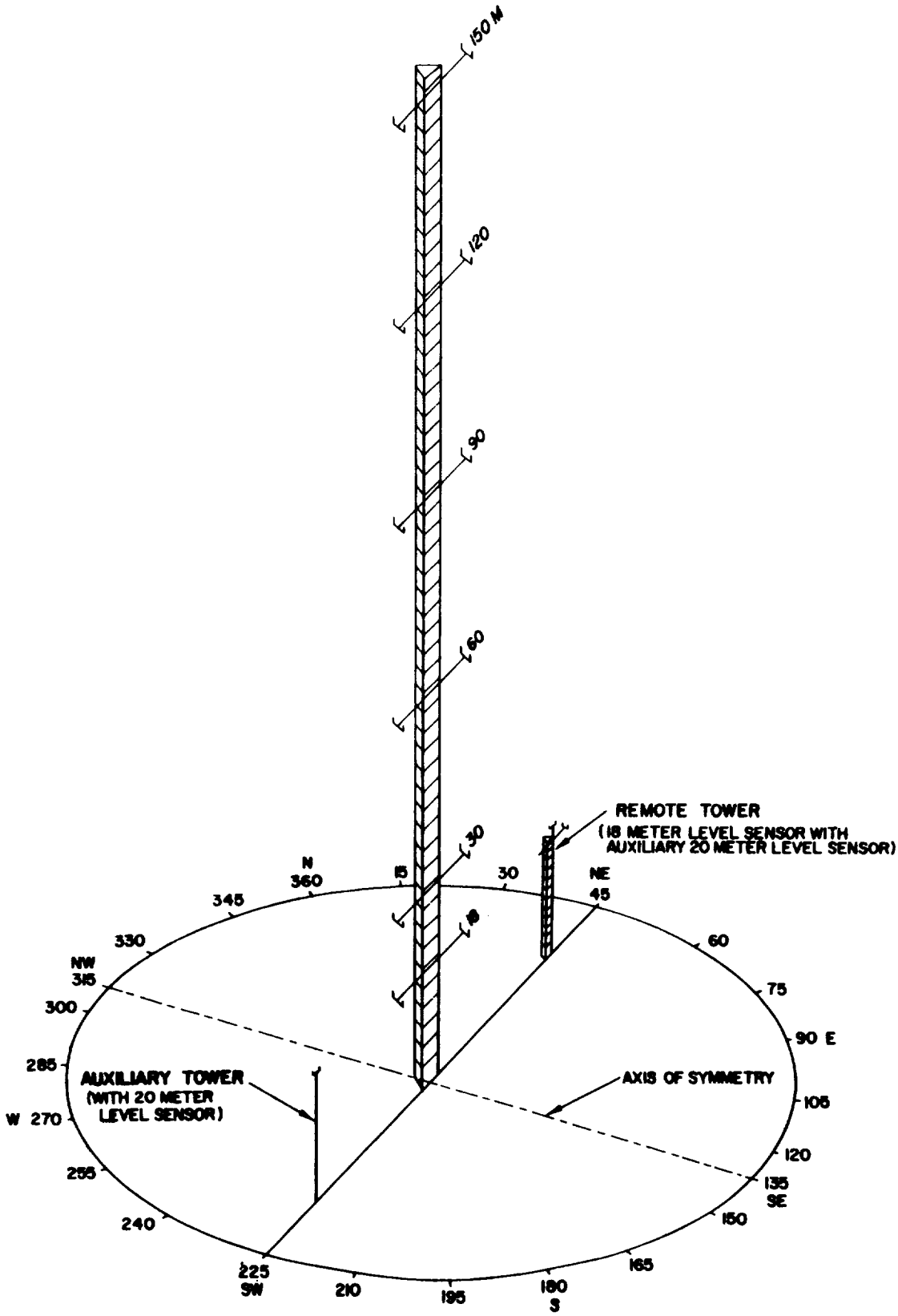

FIGURE 1-1. NASA'S 150-METER METEOROLOGICAL TOWER FACILITY AT KENNEDY SPACE CENTER, FLORIDA

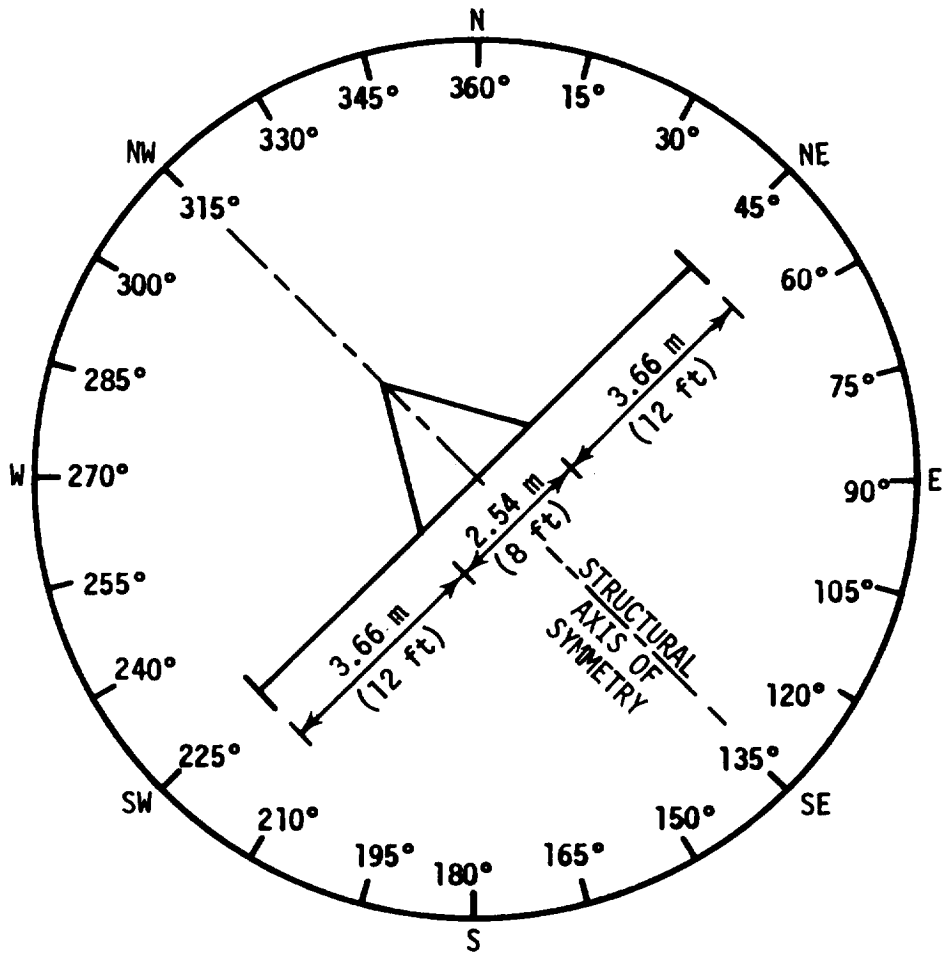

FIGURE 1-2. HORIZONTAL CROSS-SECTION OF NASA'S 150-METER METEOROLOGICAL TOWER

1.1 (Continued)

an "undisturbed" location. Theoretically, streamlines and the velocity field are computed for the flow about the tower and a comparison is then made between the flow velocity evaluated at the sensor location and the free-stream flow velocity that is used as an input to the theoretical equations.

In this study, which was primarily an experimental one, a set of correction factors for wind speed was obtained by computing ratios of measured mean wind speed to reference mean wind speed and a set of correction factors for wind direction was obtained by algebraically subtracting the measured mean wind direction from the reference wind direction. A supporting theoretical study was also performed to confirm the experimental work.

1.2 SCOPE OF DOCUMENT

Literature sources with discussions of the various methods for determining wind tower influence are reviewed in Section 2 of this document. The results from the literature review that pertain to NASA's 150-meter meteorological tower are also summarized in Section 2. Section 3 of this document presents the experimental approach (i.e., field experiment) used to determine the influence of NASA's 150-meter tower upon its wind sensor measurements. The field experiment was logically divided into a discussion of (1) the design of the experiment, (2) the data requirements, and (3) the results of the data reduction. Included in an appendix is the theoretical study in which idealized wind tower configurations were used to determine maximum tower influences at particular sensor locations for comparison with experimental results.

SECTION 2

SUMMARY OF LITERATURE ON PREVIOUS WIND TOWER INFLUENCE STUDIES

2.0 USE OF PREVIOUS INFLUENCE STUDIES

A number of wind tower influence studies were reviewed before initiating an experimental approach to determine the influence of NASA's 150-meter meteorological tower on wind measurements. Because none of these studies presented a set of correction factors that could be applied to this particular tower, the experiment presented in Section 3 was performed. However, two aspects of the reviewed literature were considered important for this study and are presented in this section: (1) the design of the experiments and the previous investigators' experiences that pertained to this work (Paragraph 2.1) and (2) the results and their associated relevance to NASA's 150-meter meteorological tower (Paragraph 2.2).

2.1 EXPERIMENT DESIGNS USED TO DETERMINE TOWER INFLUENCE

2.1.1 Types of Experiments

Two types of experiments that can be used to determine the influence that a meteorological tower's structure has on wind sensor measurements are: (1) the controlled experiment performed in the laboratory and (2) the environmental experiment performed in the field. In the controlled experiment, wind tunnels or 'towing' water tanks are used that permit the control of fluid flow speed, and also allow the scale model of the tower to be held at any desired orientation to the flow. In the environmental experiment, the full-scale wind tower is used in the natural environment where no attempt to control the environmental elements is made. For both types of experiments, the number of sensors may vary. Usually, one sensor is located in the vicinity of the tower and designated as recording the undisturbed reference flow. This reference sensor measures the free-stream speed in the wind tunnel or, in the case of the environmental experiment, the free-stream velocity of the ambient wind at some uninfluenced location away from the tower. The readings of the other sensors, located in areas where the flow is influenced by the tower, are compared to the readings of the reference sensors. The comparison is accomplished by algebraically dividing the measured mean wind speed by the reference mean wind speed thereby expressing the measured speed as a percentage of the reference speed. The comparison of wind direction is accomplished by algebraically subtracting the measured mean wind direction from the reference mean wind direction thereby giving a direction deviation angle.

2.1.2 Turbulent Versus Laminar Flow

The sensors located about either the scale model or the real tower determine whether the nature of the flow that is sensed is laminar or turbulent. A method to determine the transition between the regions of laminar and turbulent flow was used by Gill, et al., (Reference 2) on a scale model of the WJBK-TV tower (Detroit, Michigan) in low-speed wind

2.1.2 (Continued)

tunnel tests. Thirty-one metal flags were evenly spaced along a bar, and the bar was positioned upstream and downstream of the model. The flags were photographed from above, using a five-second exposure. Flags with large directional deviations over the five-second increment were used to indicate regions of turbulent flow; flags with no deviation were used to indicate regions of laminar flow. The theoretical study contained in Appendix A, Paragraph 2.0, utilized the results of this test and the technique is illustrated in Figures A-1 and A-2.

2.1.3 Speed Profile Across Wake

A low-speed wind tunnel test of a scale model of NASA's 150-meter tower, Meyer, et al., (Reference 3), determined the profile of the mean wind speed across the turbulent wake by arranging wind speed sensors in "rake" fashion and comparing their measurements to the reference speed. Hsi and Cermak (Reference 4) determined the same profile across the wake of a scale model of the White Sands Missile Range 500-foot (150-meter) meteorological tower by repositioning one speed sensor at predetermined points across the wake of the model. The results of the above two references are discussed in Paragraph 2.2.1.

2.1.4 Tower End Effects

A laboratory test to determine tower end effects was performed by Sanuki and Tsuda (Reference 5) in a "towing-water tank." The test was used to demonstrate the large vertical flow component existing at the top of a solid cylindrical stack or silo-type structure; hence the unsuitability of mounting an anemometer atop a structure of this sort was determined. Sanuki and Tsuda suggested remedying this large vertical flow component by installing the anemometer below a flat roof (for a more complete explanation, see Reference 5). This is the only report found that dealt with end effects and since this report examined the end effects atop a solid cylindrical structure, the application of these results to a triangular, lattice-type tower were limited. This particular experiment design could however be an effective method of examining the end effects of a triangular, lattice-type structure.

2.1.5 Influence at Boom-Tip Position

Investigation of the tower influence at the boom-tip position was accomplished in the wind tunnel by Vellozzi (Reference 6), Gill, et al., (Reference 2), and by Hsi and Cermak (Reference 4), by stationing a speed sensor at the anemometer's boom-tip position and comparing its measurements to the free-stream flow of the tunnel. It was convenient to perform this experiment in a wind tunnel because the scale-model tower could be rotated to predetermined orientations to the tunnel's free-stream flow with the reference sensor always located upstream of the model. An environmental experiment, patterned after wind tunnel experiments, was performed by Moses and Daubek (Reference 7) on the meteorological tower (a converted fire-lookout tower) of the Argonne National Laboratory. Five thousand (5000) hourly wind observations were reduced with data taken from all wind directions. Unfortunately, the

2.1.5 (Continued)

reference sensor, being permanently positioned away from the Argonne tower, was sometimes downstream of the tower. Dabberdt (Reference 8) performed a similar environmental experiment to determine the influence of the 128-meter Ace Tower of the Brookhaven National Laboratory. Three reference sensors were located 5.94 meters from the tower on three temporary booms that extended from the corners of the equilateral triangular tower which measured 5.5 meters on a side. Sensors were also located on each of the three booms 2.74 meters from the tower in the standard data acquisition position. Data selection was made to use the upstream sensor as the reference sensor.

2.1.6 Description of Influence Field

An environmental experiment was used by Thornthwaite, et al., (Reference 9), to study the characteristic disturbance of the natural airflow caused by the Argus Island tower (a Texas tower) in order to find a suitable position for installing outrigged micrometeorological instruments. A permanent reference sensor was located approximately 18 meters above the tower. Six anemometers, on mobile rigging that could be installed rapidly at various predetermined points, were repositioned about the tower. The measurements of the mobile sensors were divided by the reference measurement to provide a ratio of wind speed about the tower to reference speed. Analysis of the ratios with respect to their positions about the tower gave a description of the tower influence field. This experimental technique is especially applicable for the study of a tower that experiences prevailing winds with a pronounced wind direction frequency. NASA's 150-meter meteorological tower does not experience the necessary prevailing wind direction to permit an experiment of this design.

2.2 APPLICABILITY OF REVIEWED LITERATURE TO NASA's 150-METER METEOROLOGICAL TOWER

The design, structure, and hardware of individual meteorological towers vary considerably. This difference in structure and hardware necessitates individual influence studies for the individual towers. There is, however, some applicability of results of one tower study to another tower where design and terrain similarities exist.

2.2.1 Composite Influence

It is important to note that the composite influence is due to all of the structure and hardware on the tower. The composite influences that are presented in previous studies are summarized in Table 2-I as the average increase of wind speed abreast of the tower (i.e., 120-150° from the direction of the wind) and the average decrease of wind speed in the wake of the tower.

The first five studies in Table 2-I are the most applicable to NASA's 150-meter meteorological tower since triangular lattice-type structures were tested. The remaining two studies involve other types of structures

TABLE 2-I. SUMMARY OF TOWER INFLUENCE STUDIES

NUMBER	STUDY (BY AUTHOR)	TYPE OF STRUCTURE	TYPE OF TEST	AVERAGE INCREASE ABREAST* OF TOWER (%)	AVERAGE DECREASE IN TOWER WAKE (%)
1	Gill, Olsson and Suda (Reference 2)	Triangle, Lattice	Wind Tunnel	5 - 10	25 - 35
2	Meyer, Reese, and Ziler (Reference 3)	Triangle, Lattice	Wind Tunnel	3 - 10	30 - 40
3	Hsi and Cermak (Reference 4)	Triangle, Lattice	Wind Tunnel	6	30 - 35
4	Vellozzi (Reference 6)	Triangle, Lattice	Wind Tunnel	1 - 2	20
5	Dabberdt (Reference 8)	Triangle, Lattice	Environment	19	35
6	Moses and Daubek (Reference 7)	Square, Lattice	Environment	20 - 30	26 - 45
7	Borovenko, et. al., (Reference 10)	Cylinder, Solid	Environment	2.5 at 3 tower radii	-------

* 120 - 150° from wind direction; yet outside of wake.

2.2.1 (Continued)

(a fire tower and a solid cylindrical tower) and are presented for completeness. From the first five studies, the increases of wind speed abreast of the tower varied from 1 to 2 percent above the free-stream wind speed in one study to 19 percent in another. The decreases of wind speed in the wake varied from 20 to 40 percent below the free-stream wind speed. Moses and Daubek (Reference 7 and study number 6 on Table 2-I) studied the variation of the influence field in the wake with changes of wind speed and found an inverse relationship between the percentage decrease in the tower wake with a change in the wind speed (from 45 to 26 average percentage decrease with an increase of speed from 0-4 mph to 10-14 mph).

Wherein possible the results presented in Table 2-I are for boom lengths of 1 1/2 D (where D is the characteristic diameter or length of the side of the tower). Vellozzi (Reference 6) determined that at high wind speeds (29-69 mph or 13.7 to 32.9 meters per second) boom length has little bearing upon influence; whereas, Gill, et al., (Reference 2) determined that for lower wind speeds (8-9 mph) the boom should be no less than 1D. The Gill report suggested mounting the sensors on opposing sides of the tower to insure a sensor on the least-influenced, upwind side of the tower. They also suggested the configuration shown in Figure 2-1 as opposed to Figure 2-2. In addition, Gill recommended mounting the sensors at levels of minimum tower density (i.e., above or below horizontal cross members). NASA's 150-meter meteorological tower has dual booms oriented on opposing sides of the tower.

The first four studies listed in Table 2-I are wind tunnel studies using modeled sections of existing towers. In correlating wind tunnel results to the prototype tower, Hsi and Cermak (Reference 4) verified by comparing perturbed to unperturbed flow in a wind tunnel that the higher turbulence level found in the environment "does not have a significant effect on the wind velocity defect (influence) in the wind tunnel." In a later paper, Cermak and Horn (Reference 11) amplified this result by noting that "... the Reynold's number differs by less than one order of magnitude for the model and prototype tower ...." Meyer, et al., (Reference 3) showed a Reynolds number range for their scaled model that departed by no more than an order of magnitude from the Reynold's number range for the full scale model; however, they suggest the use of a full-scale wind tunnel test to verify their results in the wake region, due to extreme shadow effects.

Of the reports tabulated in Table 2-I, only Vellozzi (Reference 6) attempted to determine the deviation of the wind direction measurement with respect to wind direction. Vellozzi measured deviations ("reference" minus "influenced" direction sensor) of -1 to -7 degrees.

2.2.2 Component Influence

It is difficult to determine the exact influence of each of the components on the tower (i.e., catwalks, conduits, guy wires, and booms). Meyer, et al., (Reference 3) attempted to determine these tower component's

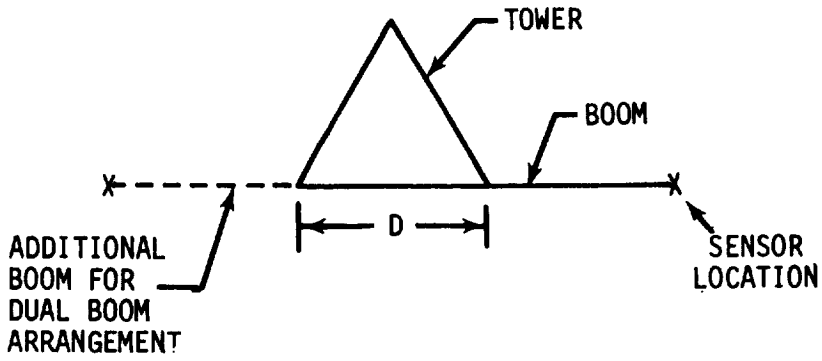

FIGURE 2-1. BOOM ARRANGEMENT RECOMMENDED BY GILL, ET AL., (REFERENCE 2).

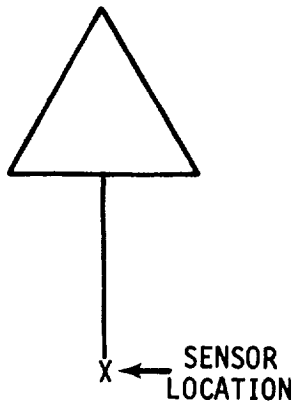

FIGURE 2-2. BOOM ARRANGEMENT TESTED BY GILL, ET AL., (REFERENCE 2).

2.2.2 (Continued)

influence in altering speeds in the wake of the tower, thereby, determining their approximate percentage of the total composite tower influence. The catwalk increased the size of the wake as seen by a "tuft grid" placed downstream of the tower; and, generally decreased the speeds in the wake directly downstream by an amount comparable to the size of the major structural members. They also determined that:

1. "... the presence of the two major conduits on the boom side of the tower has significant effect on the velocity distribution, [downstream]."

2. "Cable [guy wire] effects are evident in most cases [in the speeds of the wake] but considerably less, and perhaps insignificant at the higher velocity conditions."

3. "The effects of cable [guy wire] attachment [i.e., level and angle of attachment to the tower] is not particularly significant at least for those cases tested."

Vellozzi (Reference 6), using the same tower model tested by Meyer (Reference 3), performed high speed wind tunnel tests (29 to 69 mph) and found decreased influence in the wake of the tower with catwalk as compared to the tower without catwalk (an average decrease of 13 percent across the wake for tower with catwalk versus 18 percent for tower alone). No explanation is offered for this seemingly unusual result. Tests to determine the effect of the booms on the flow were performed by Borovenko, et al., (Reference 10) and by Dmitriyev (Reference 12). About a 16 percent increase in speed would be recorded if the anemometer were placed directly over the boom at a distance of 1.25 boom diameters. Therefore, from Borovenko's results, it was felt that the sensors should be on cross arms at a distance greater than 2 boom diameters from the centerline of the boom. In addition, a paper by Sanuki, et al., (Reference 13) reported that about a two percent increase in wind speed would be experienced by an anemometer when installed at 3.5 boom diameters from the centerline of the boom.

Borovenko, et al., (Reference 10) and Thornthwaite, et al., (Reference 9) have found local stagnation areas immediately windward of large solid obstructions on the tower such as elevator pulley housings, electrical junction boxes, etc. This stagnation area is not large with respect to the solid obstacle; however, it would be unwise to place a sensor immediately windward of such a solid obstacle.

2.2.3 Literature Summary

In condensing the findings and conclusions of previous studies for their relevance to this study, it has been found that:

1. An environmental study to determine the influence of NASA's 150-meter meteorological tower should be carried out to verify the results of the two wind tunnel studies that used the scale model of NASA's tower, Meyer et al., (Reference 3), and Vellozzi (Reference 6), by

2.2.3 (Continued)

comparing these results to the fully rigged tower.

2. An environmental study should be carried out to determine if the increased turbulence level of the ambient environment differs from the wind tunnel results.

3. The measuring wind sensors should be located at least 1 1/2 D (D=tower width) from the tower and, preferably, oriented such that the sensor is always on the windward side of the tower, and in the plane of the tower face. One method of achieving this is to have a dual boom/dual sensor arrangement at every level and a wind direction selecting device to continuously decide which sensor to monitor. Further, it is preferable that the sensor not be mounted immediately upwind of a solid obstruction on the tower nor at a level of maximum tower density, where horizontal cross members exist.

4. For environmental influence studies, the reference sensor should be "well away from the tower" (greater than 6D) yet not so far that it does not sense the same mean wind. It is also preferable to have the reference sensor upwind of the tower. The reference sensor should, of course, be located at the same level as the measuring sensor, or compensation made for a change in height.

5. The sensors should be mounted on cross arms and positioned with respect to the boom at a distance greater than 3.5 boom diameters away from the boom.

6. Sensor placement with respect to guy wire location is insignificant. Conduits can pose a notable disturbance in the wake region. Catwalks can also pose considerable influence in the size of the wake.

SECTION 3

EXPERIMENTAL APPROACH TO THE STUDY OF WIND TOWER INFLUENCE

3.0 BACKGROUND

The controlled, wind tunnel experiments that were performed on a scale model of NASA's 150-meter meteorological tower by Meyer, et al., (Reference 3) and Vellozzi (Reference 6) tested a very "clean" model of a section of the tower. Without the full outfitting of hardware that exists on the actual tower, these tests have no more relevance to NASA's tower than does the scale model tested by Gill, et al., (Reference 2) that more closely approximates the porosity of but differs in design from NASA's 150-meter prototype tower. In addition, atmospheric turbulence considerations have generated concern over the representativeness of results from wind tunnel model experiments to a full-scale tower. The above two aspects of wind tunnel experiments and their applicability to NASA's 150-meter tower led to the initiation of this environmental experiment. This experiment was designed primarily to determine whether or not NASA's 150-meter tower significantly influences the wind measurements obtained from the sensors mounted upon it, and if so, to determine the means to uniquely correct the measured wind speeds and directions to approximate the free-stream wind. These two determinations were performed by computing correction factors in standard wind tunnel fashion.

The physical considerations at the facility, sensor locations, and data reduction procedures were elements incorporated into the design of this experiment and are discussed in Paragraph 3.1. The data acquired for the experiment are discussed in Paragraph 3.2 and the experimental results are discussed in Paragraph 3.3. In addition, an attempt was made to determine the influence that the tower has on turbulence measurements and is reported on in Paragraph 3.4.

3.1 EXPERIMENT DESIGN

The design of this experiment developed from: (1) physical considerations at the facility as presented in Paragraph 3.1.1, (2) the establishment of reference sensors as discussed in Paragraph 3.1.2, and (3) the methods used to reduce the data as discussed in Paragraph 3.1.3.

3.1.1 Physical Considerations of NASA's 150-Meter Meteorological Tower Facility

Numerous elements were taken into consideration in the design of this experiment including an attempt to incorporate wind tunnel techniques wherever possible. The physical considerations of NASA's 150-meter meteorological tower facility itself were major factors in the experiment design. The following facility features were assets to the study:

1. An Ampex FR-1200 magnetic tape system with thirteen channels for data records and one channel for the time record permits the acquisition

3.1.1 (Continued)

of analog data which can be digitized at 10 samples per second, if necessary. This computer oriented input permits the assimilation of large amounts of data.

2. Sensors are located on the northeast and southwest sides of the tower, and data can be recorded on magnetic tape from both sides simultaneously (Figure 1-2).

3. The open field location of the tower facility permits the temporary positioning of an auxiliary sensor.

The following constraints were incorporated into the experiment design:

1. The recent establishment of this facility limited the quantity of hourly winds available so that a study similar to the Moses and Daubek experiment, based on climatologically summarized data, (Reference 7) could not be accomplished.

2. The experiment should not interfere with the normal data acquisition program carried on at the facility.

3. A minimum of additional equipment was preferred in order to curtail expense and to avoid time-consuming equipment construction and installation.

4. The obvious lack of flexibility in tower orientation and flow speed control of an environmental experiment versus one performed in the wind tunnel required that an extended period of data acquisition be allotted for suitable variations in wind speed and direction to occur.

The second limiting consideration above required that a rapid and accurate method of converting the operations at the facility from one experimental mode to another be utilized without interfering with normal data acquisition. The normal data acquisition is performed by recording the data on strip chart recorders. The channels of the analog tape recorder were wired in parallel with the strip chart recorders so that the tape recorder's operation would not interrupt the normal data acquisition on the strip charts. Computer-type patchboards were then employed to perform the change of experimental operating modes. Individual patchboards were programmed for each desired experiment and the simple replacement of the board on the patchpanel was all that was required to alter the mode of operation at the facility.

3.1.2 Reference Sensors

In order to emulate wind tunnel experiments for the reference measurements, two sensor locations were established away from the tower. For one reference sensor location, the remote tower, 18 meters northeast of the main tower (see Figure 1-1), was used. Since the remote tower has a sensor at

3.1.2 (Continued)

the 18-meter level that was probably subject to some interference from the structure of the remote tower itself, the reference sensor was located on a pole at the 20-meter level, 2 meters above the remote tower. For a second reference sensor, an auxiliary tower with a sensor at the 20-meter level was located 18 meters southwest of the main tower, thereby providing a mirror image to the northeast reference sensor (see Figure 1-1). This southwest reference sensor was also pole-mounted to guard against undue structural influence. The measured mean wind direction was used to determine which of these sensors was upwind of the tower and was to be used as the "reference sensor."

3.1.3 Data Reduction

Influence factors: One objective of this study was to establish, if necessary, a set of influence factors to be used as correction factors for the wind speed and direction measurements made by sensors on the tower. These influence factors were computed by comparing the mean speed and direction measurements from the 18-meter level to the mean speed and direction measurements of the established reference sensors. These factors were computed for speed values by:

$$\text{Influence Speed Ratio} = \frac{S_M}{S_R} \tag{3-1}$$

and for direction values by:

$$\text{Influence Direction Deviation} = D_R - D_M \tag{3-2}$$

where S and D are wind speed and direction and the subscripted M and R denote the measuring and referencing sensors. The measuring sensor was taken to be the normally operating sensor located on the main tower. From Figure 3-1 the reference sensors are at Stations 3 and 6 and the measuring sensors are at Stations 4 and 5. Only one reference sensor was used at any one time. It was always the sensor on the windward side of the tower and was determined by inspecting the data before processing. The measuring sensors at Stations 4 and 5 were always compared to the same reference sensor.

Comparative Factors: To increase the volume of data used in this study, it was convenient to assume that an axis of symmetry existed in the large-scale influence field and was collinear with the structural axis of symmetry of the tower (Figure 1-2). To verify this assumption of an axis of symmetry, a comparison was made between winds measured by sensors on opposing sides of the tower. The comparison was made specifically between windward and leeward sensors and was computed for speed values by:

$$\text{Comparative Speed Ratios} = \frac{S_L}{S_W} \tag{3-3}$$

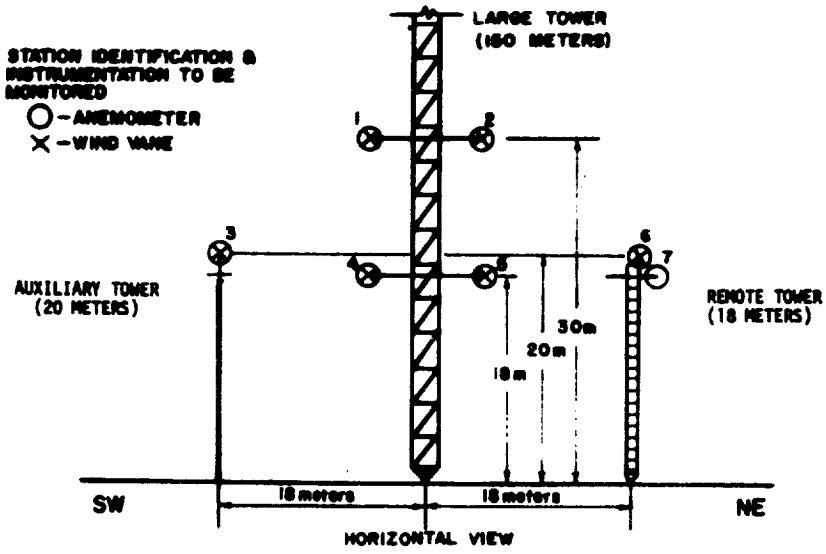

FIGURE 3-1. SENSORS MONITORED FOR THE "A" TESTS - LOWER LEVEL

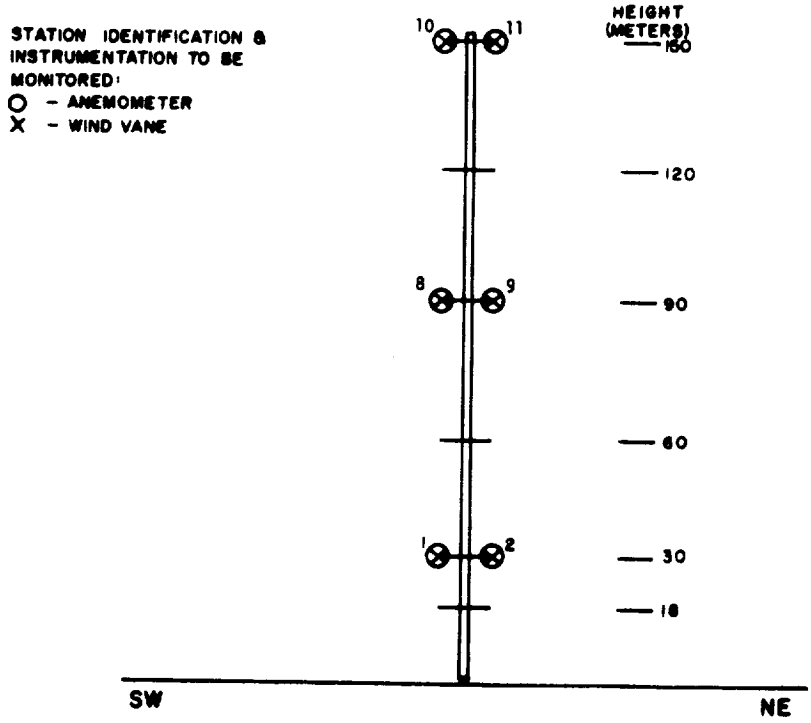

FIGURE 3-2. SENSORS MONITORED FOR THE "B" TESTS - UPPER LEVEL

3.1.3 (Continued)

and for direction values by:

$$\text{Comparative Direction Deviations} = D_W - D_L \qquad (3\text{-}4)$$

where S and D are speed and direction and the subscripted W and L denote windward or leeward sensor.

If the patterns of ratios and deviations computed for winds blowing from one side of the tower were reflections of the patterns for winds from the other side, then an axis of symmetry existed. This permitted an overlay of data from the southwestern half of the compass onto the northeastern half which, of course, reflected an increase in the data volume. From Figure 3-1, it can be seen that for winds blowing from the northeastern half of the compass, the northeast sensor (at Station 2) was the windward sensor and the southwest sensor (at Station 1) was the leeward sensor for use in Equations 3-3 and 3-4. For winds blowing from the southwest half of the compass, the windward/leeward designation was reversed. This comparison was carried out at the 30-meter level where the data volume was the greatest.

Since it was impractical to establish a reference sensor at every recording level on the tower, it was assumed that the influence fields at all levels are the same. This second assumption permits the use of the influence factors, which were derived at the 18-meter level, at all levels of the tower. This assumption is, in essence, the same assumption made in wind tunnel experiments when a scale model of the tower is tested in the test chamber.

The same comparative factors in Equations 3-3 and 3-4 were used to verify this second assumption. The comparative ratios and deviations computed for any one level were compared to those at the other levels to determine if overall similarity existed. This can be determined in Figures 3-1 and 3-2 in that the comparative factors were computed using measurements at the 30-meter level (Figure 3-1, Stations 1 and 2), at the 18-meter level (Figure 3-1, Stations 4 and 5), at the 90-meter level (Figure 3-2, Stations 8 and 9), and 150-meter levels (Figure 3-2, Stations 10 and 11). Similarity between the comparative factors for the 30-meter level to the other levels was used to verify that the structural and equipment differences existing at the levels have minimal influence. Thus, the structural and equipment differences did not alter the total influence sufficiently to negate the use at all levels of the 18-meter-level-derived influence ratios.

3.2 EXPERIMENTAL DATA

Data for the study were acquired from March 16, 1967 to June 12, 1968 (15 months).

For purposes of labeling the data, an array of wind speeds and directions was used (see Table 3-I). Speeds were incremented by two meters per second

TABLE 3-I. DATA ARRAY FOR WIND TOWER INFLUENCE STUDY

Test Duration: 10 minutes (600 seconds)

Wind Direction Ranges* (Degrees)	Wind Speed Ranges* (m/sec)				
	2 - 4	4 - 6	6 - 8	8 - 10	>10
360 - 30	Test 11	Test 12	Test 13	Test 14	Test 15
30 - 60	Test 21	Test 22	Test 23	Test 24	Test 25
60 - 90	Test 31	Test 32	Test 33	Test 34	Test 35
90 -120	Test 41	Test 42	Test 43	Test 44	Test 45
120 -150	Test 51	Test 52	Test 53	Test 54	Test 55
150 -180	Test 61	Test 62	Test 63	Test 64	Test 65
180 -210	Test 71	Test 72	Test 73	Test 74	Test 75
210 -240	Test 81	Test 82	Test 83	Test 84	Test 85
240 -270	Test 91	Test 92	Test 93	Test 94	Test 95
270 -300	Test 101	Test 102	Test 103	Test 104	Test 105
300 -330	Test 111	Test 112	Test 113	Test 114	Test 115
330 -360	Test 121	Test 122	Test 123	Test 124	Test 125

*Wind speed and direction ranges are to be as determined by the windward sensors at the 30-meter level of the 150-meter tower.

3.2 (Continued)

and directions by thirty degrees. Test numbers were assigned to each element of the array thereby referencing their position in the array. This test number was subsequently assigned to the data sequence that was recorded when the mean wind was blowing with that speed and from that direction. The data sequences were called test cases and several test cases could have been taken for any element in the array.

The test cases were recorded for ten-minute intervals using the analog tape recorder. This analog tape was digitized at a one-second time increment into a data sequence that was 600 seconds long with one digital data record for each second.

The study required the simultaneous monitoring of twenty stations; however, the analog tape recorder has only thirteen data channels. For this reason, two sets of tests (designated "A-tests" and "B-tests") were recorded for the lower and upper sensors on the tower (see Figures 3-1 and 3-2) in order to accommodate all twenty sensors. The 30-meter level sensors were common to both sets. There was a data array like Table 3-I for both "A" and "B" tests.

There were 60 elements in each of the A and B data arrays. Fifty-three of the elements in the A array and 48 of the elements in the B array were filled during the fifteen month data acquisition period. Due to the redundancy of test cases, a total of 167 A and B type tests were processed for this study.

The normal climatological wind data obtained at the facility is a ten-minute mean wind speed and direction obtained from five minutes before to five minutes after the hour; for this reason, a ten-minute mean wind speed and direction data collection period was used in this study. In this way, operational type data were used to compute correction factors. In some instances, data were unrepresentative of the mean winds at the reference and tower sensor locations and had to be deleted. These cases were determined by compiling speed and direction frequency distributions for each sensor in each test from the one-second data; and then deleting cases having unrepresentative mean winds, such as well-separated bimodal distributions or highly skewed distributions.

3.3 EXPERIMENTAL RESULTS

The three aspects of the experimental results for which the experiment design was established are presented as follows: (1) verification of the bilateral symmetry assumption (Paragraph 3.2.1), (2) verification of the similarity of influence at all levels assumption (Paragraph 3.2.2), and (3) determination of influence factors (Paragraph 3.2.3). These results are presented separately since the wind speed and wind direction are independent measurements.

3.3.1 Verification of Bilateral Symmetry Assumption

The 30-meter level was used as the level to verify the bilateral symmetry assumption because these sensors were monitored for both the A and B type tests thus yielding the most data.

Figure 3-3 presents the comparative speed ratios (dots) for the 30-meter level (Figure 3-1, Stations 1 and 2). The ratios of Figure 3-3 are plotted versus the direction of the leeward sensor and a Cartesian coordinate grid is used to make the comparison about the 135-degree radial (structural axis of symmetry) more convenient. Superimposed over the computed data points of Figure 3-3 is an interpolated mean ratio line (solid line). This type data does not lend itself to the more standard types of statistical summarization because the independent variable of direction is not evenly incremented. This is an advantage to wind tunnel researchers. The dashed line superimposed on the computed data points is the mirror image, or transform, of this mean ratio line (solid line), projected across the structural axis of symmetry (i.e., the northwest-southeast line). There is a 7 percent departure of the mean ratio line to the transformed mean ratio line in the wake region of 10 to 50 degrees and 220 to 260 degrees. There is less than a 2 percent departure in the regions from 60 to 215 degrees and 280 to 360 degrees.

The comparative direction deviations (dots) are presented in Figure 3-4 with their mean deviation line (solid line) and its mirror image line (dashed line) for comparisons about the structural axis of symmetry. The mirror image line is inverted in order that a positive deviation on one side of the structural axis of symmetry becomes a negative deviation for the complementary direction on the other side. The largest departure between the two deviation lines (4 degrees) occurs at 135 degrees where the selection of "which side of the tower was to be the leeward side" had to be made. Another region of interest is in the vicinity of 225 degrees where the northeast sensor (Figure 3-1, Station 2) was in the wake and yielded erratic results differing by more than 30 degrees.

With only a 7 percent departure in the comparative ratios and a maximum of 4 degrees departure in comparative deviations, it was assumed that the influence fields are bilaterally symmetrical about the structural axis of symmetry of the tower and that the asymmetries in the placement of hardware, cables, conduits, and elevator tracks do not sufficiently alter the flow so as to induce asymmetries in the flow field.

3.3.2 Verification of Similarity of Influence at all Levels

The mean ratio and mean deviation line (solid line) for the 30-meter level are reproduced on the Figures 3-5 (a, b, c) and 3-6 (a, b, c) which present the comparative speed ratios and direction deviation (dots), respectively, for the 18, 90, and 150-meter levels.

As seen in Figure 3-5 (a, b, c), the mean ratio line for the 30-meter level closely approximates the trend of the comparative ratio points computed for

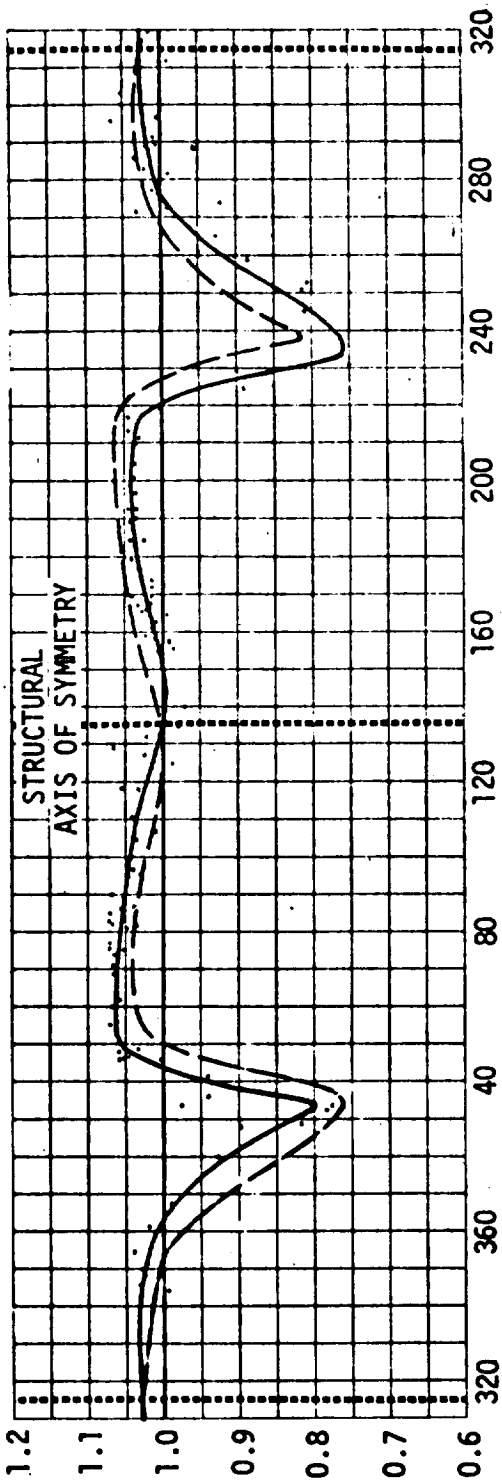

FIGURE 3-3. COMPUTED COMPARATIVE SPEED RATIOS (DOTS) AND MEAN SPEED RATIOS (SOLID LINE) FOR 30-METER LEVEL. THE TRANSFORMED MEAN SPEED RATIO (DASHED LINE) IS OVERPLOTTED TO FACILITATE THE VERIFICATION OF THE BILATERAL SYMMETRY ASSUMPTION.(Data acquired at 150-meter meteorological tower facility at Kennedy Space Center, Florida, from March 16, 1967, to June 12, 1968.)

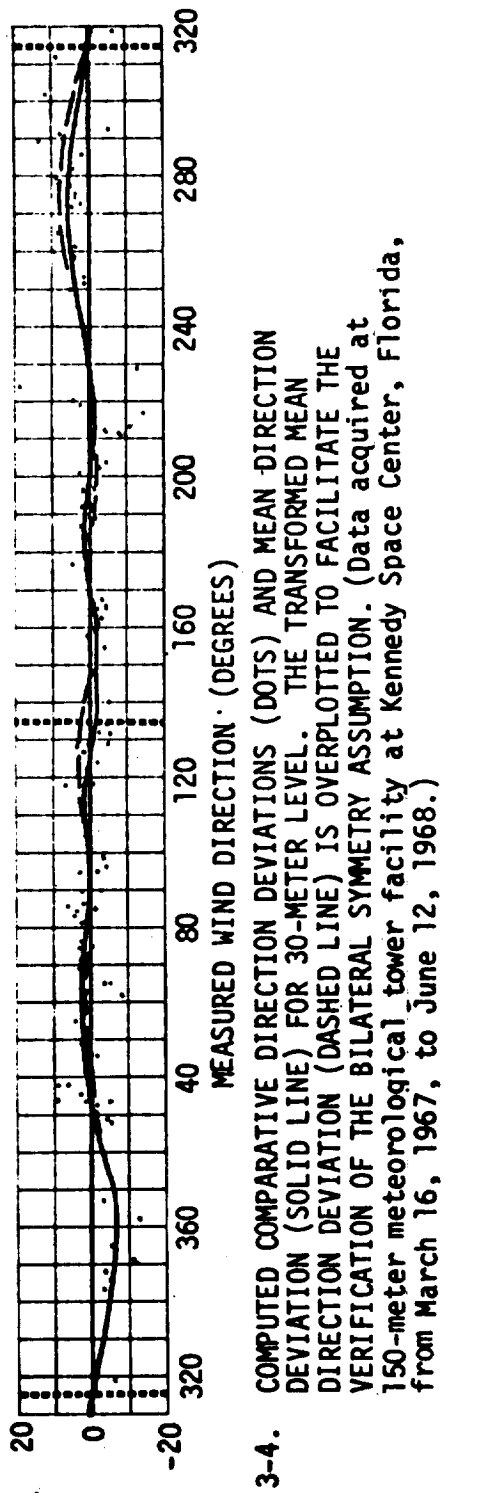

FIGURE 3-4. COMPUTED COMPARATIVE DIRECTION DEVIATIONS (DOTS) AND MEAN DIRECTION DEVIATION (SOLID LINE) FOR 30-METER LEVEL. THE TRANSFORMED MEAN DIRECTION DEVIATION (DASHED LINE) IS OVERPLOTTED TO FACILITATE THE VERIFICATION OF THE BILATERAL SYMMETRY ASSUMPTION. (Data acquired at 150-meter meteorological tower facility at Kennedy Space Center, Florida, from March 16, 1967, to June 12, 1968.)

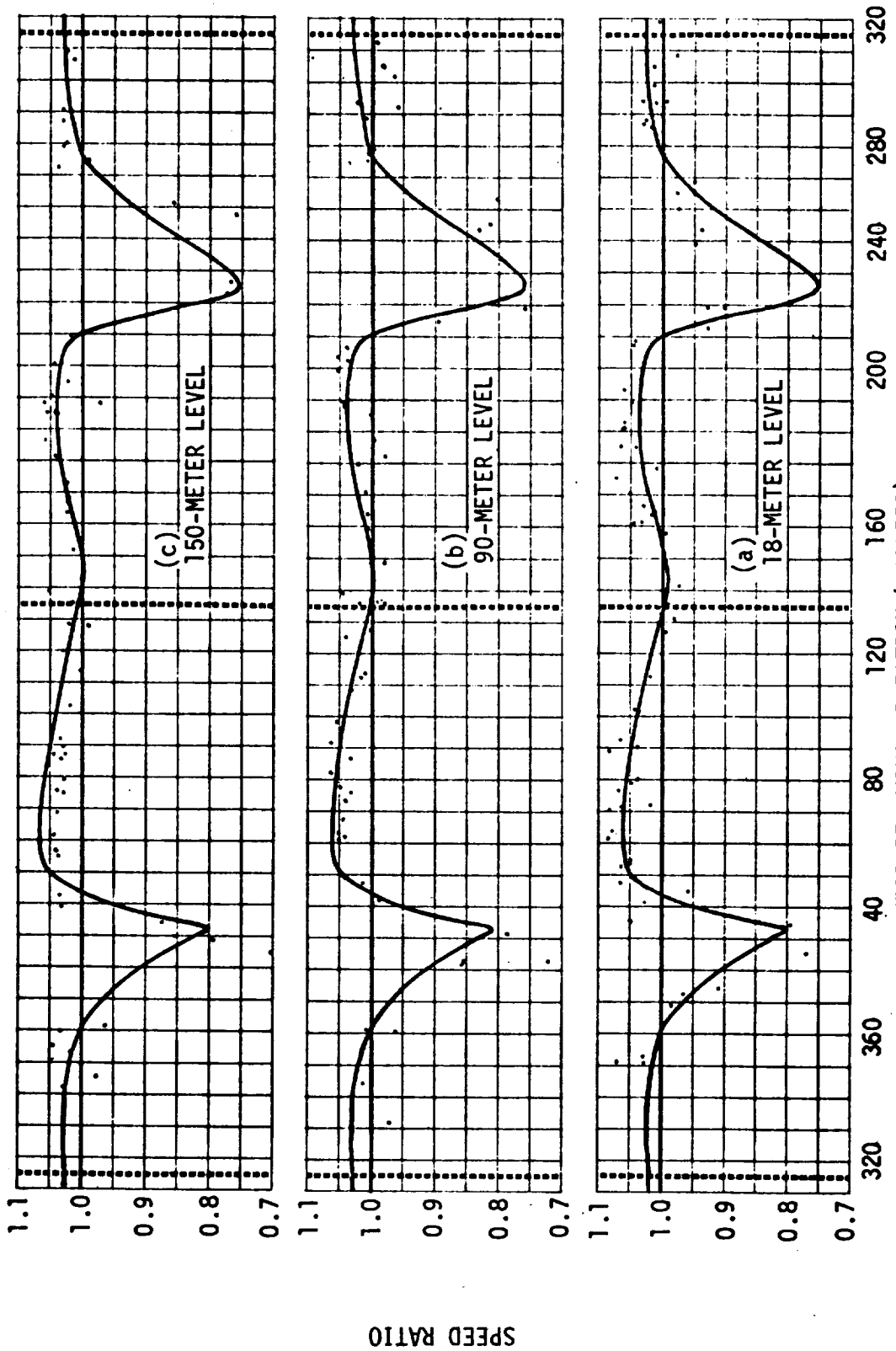

FIGURE 3-5 (a,b,c). COMPUTED COMPARATIVE SPEED RATIOS (DOTS) FOR THE 18, 90, AND 150-METER LEVELS WITH THE 30-METER LEVEL MEAN SPEED RATIOS (SOLID LINE) OVERPLOTTED TO FACILITATE THE VERIFICATION OF SIMILARITY OF INFLUENCE AT ALL LEVELS. (Data acquired at 150-meter meteorological tower facility at Kennedy Space Center, Florida, from March 16, 1967, to June 12, 1968.)

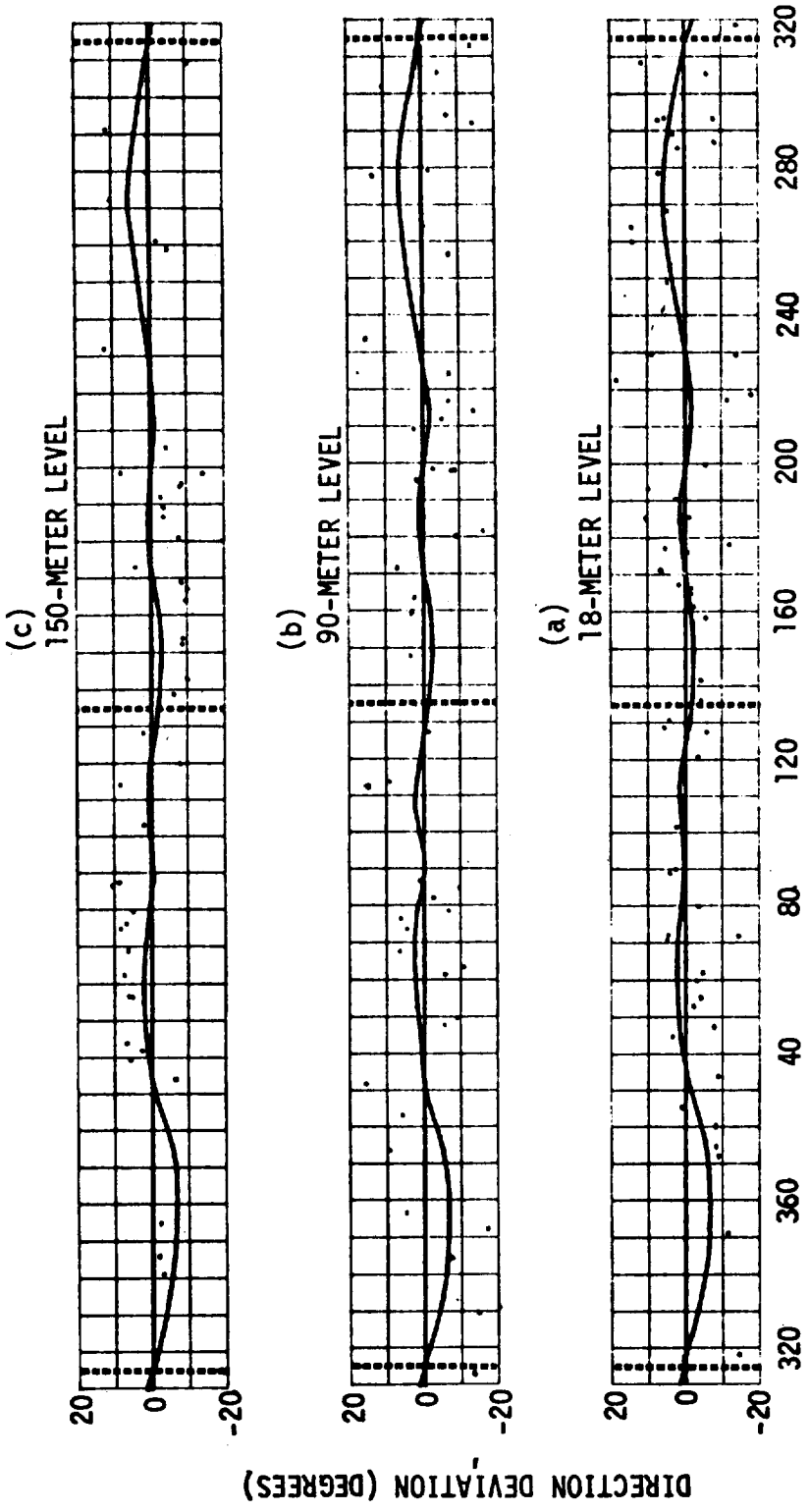

FIGURE 3-6 (a,b,c). COMPUTED COMPARATIVE DIRECTION DEVIATIONS (DOTS) FOR THE 18, 90, AND 150-METER LEVELS WITH THE 30-METER LEVEL MEAN DIRECTION DEVIATION (SOLID LINE) OVERPLOTTED TO FACILITATE THE VERIFICATION OF SIMILARITY OF INFLUENCE AT ALL LEVELS. (Data acquired at 150-meter meteorological tower facility at Kennedy Space Center, Florida, from March 16, 1967, to June 12, 1968.)

3.3.2 (Continued)

the other levels. The largest departure outside the wake region (-2 percent) occurs in the vicinity of 70 degrees at the 150-meter level (Figure 3-5 [c]). Within the wake region, there are variations as large as 15 percent for individual data points.

The direction deviations, presented in Figure 3-6 (a, b, c), do not present such a conclusive verification of similarity at all levels. The correspondence of the computed deviations at the 18-meter level to the 30-meter level mean deviation line (Figure 3-6 [a]) is good, except in the wake region at 225 degrees where the dispersion is large. The computed direction deviation points of the 90-meter level (Figure 3-6 [b]) have a large dispersion and do not allow conclusions to be drawn that have any significant degree of confidence associated with them. For the 150-meter level (Figure 3-5 [c]), the direction deviation points fit the pattern of the 30-meter level mean deviation line; however, there is about 6 degrees greater amplitude in the vicinity of 70 and 150 degrees. With a fuller investigation of the end effects of the tower, this increased amplitude may be explained.

Based on the good fit of the comparative speed ratios at all levels and the fair fit of the comparative direction deviations at the 18 and 150-meter levels, the assumption of similarity of influences at all levels is considered valid. The importance of this assumption to all tower influence studies, both wind tunnel and environmental, is that it permits the determination of correction factors at some level of the tower, or for some scaled section of the tower, that can then be used for all other levels of the tower.

3.3.3 Determination of Influence Factors

Influence speed ratios and influence direction deviations (dots) are presented for the southwest and northeast sensors at the 18-meter level (i.e., Stations 4 and 5, respectively) in Figures 3-7 and 3-8 along with their respective mean ratios and mean deviations (solid lines). In addition, in Figure 3-8, the mean ratio and mean deviation for Station 4 (dashed lines) is transposed and overplotted to reverify the bilateral symmetry assumption. There is good fit for both the ratios and deviations.

Figures 3-9 and 3-10 present the composite influence speed ratios and influence direction deviations for both northeast and southwest sensors at the 18-meter level (Stations 4 and 5). The ratios and deviations for the southwest sensor (Station 4) have been transposed such that Station 5 now represents the sensor in the influenced position near the tower and will be compared to the reference sensor. Also, the figures are plotted on polar grid paper to facilitate the comparison of the influence patterns with the orientation of the wind tower to the measured wind direction. The tower (with only the northeast boom) is superimposed in the center of the figure for this purpose. The wind directions in parentheses are those to be used

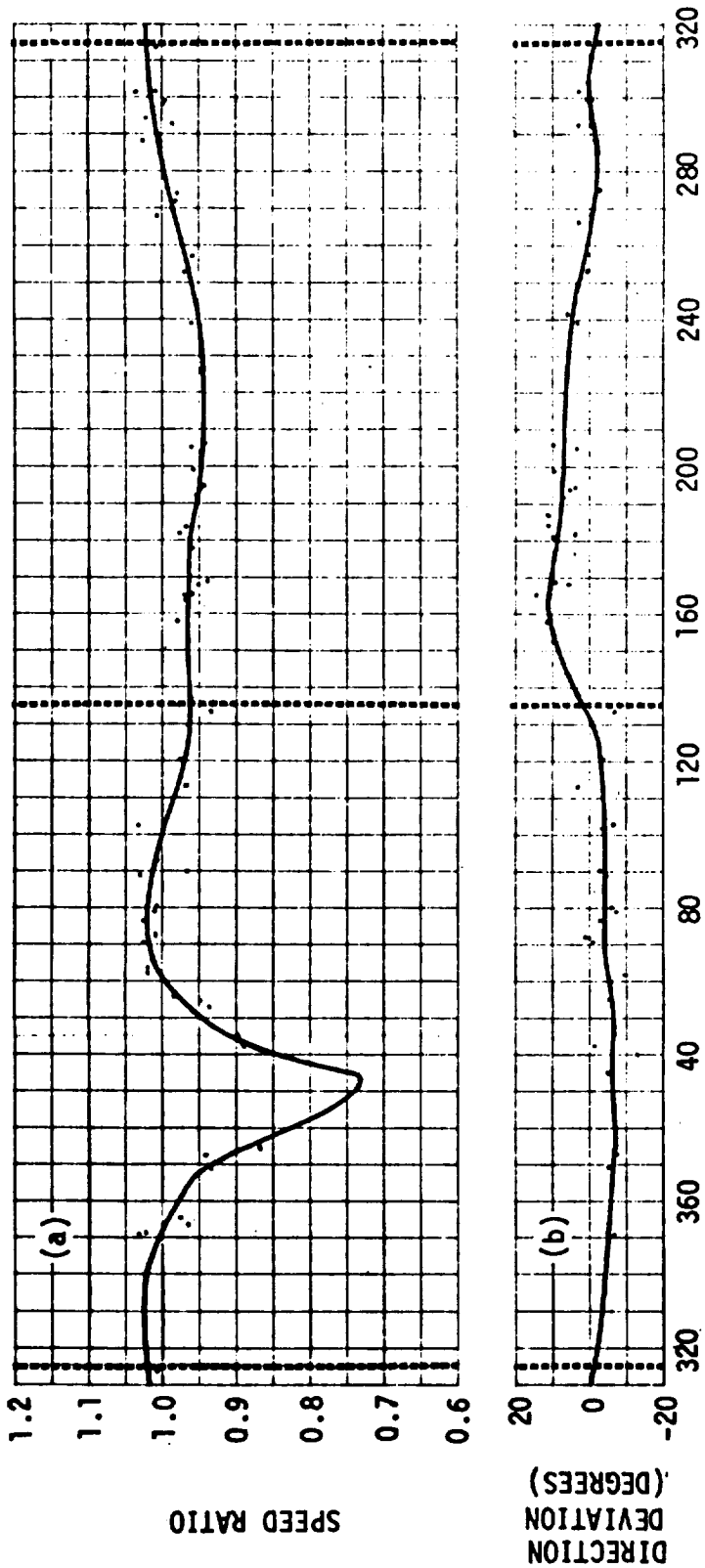

FIGURE 3-7 (a, b). COMPUTED INFLUENCE SPEED RATIOS (DOTS) AND DIRECTION DEVIATIONS (DOTS), RESPECTIVELY, WITH MEAN SPEED RATIO AND DIRECTION DEVIATION (SOLID LINE) FOR STATION 4. (Data acquired at 150-meter meteorological tower facility at Kennedy Space Center, Florida, from March 16, 1967, to June 12, 1968.)

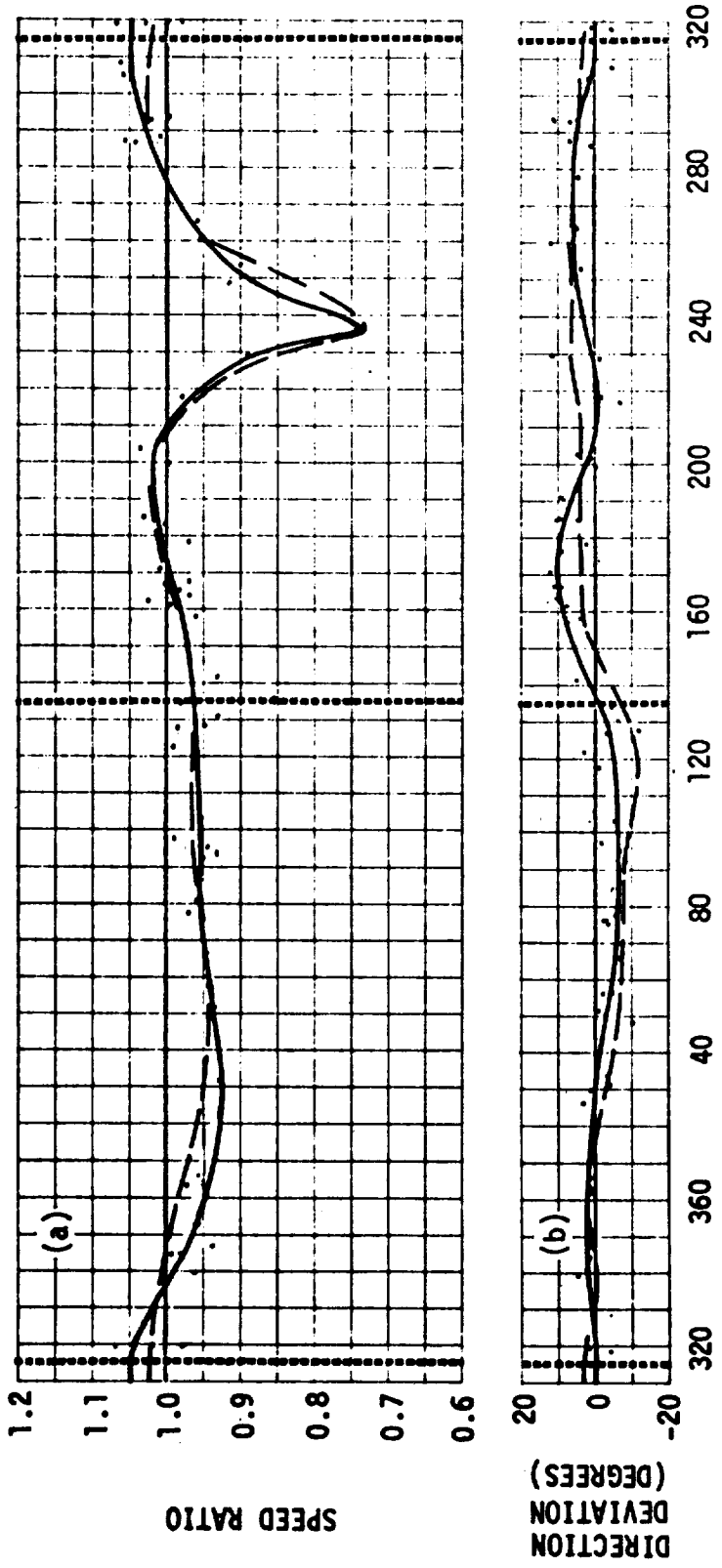

FIGURE 3-8 (a, b). COMPUTED INFLUENCE SPEED RATIOS (DOTS) AND DIRECTION DEVIATIONS (DOTS), RESPECTIVELY, WITH MEAN SPEED RATIO AND DIRECTION DEVIATION (SOLID LINES) FOR STATION 5. TO FACILITATE A REVERIFICATION OF THE BILATERAL SYMMETRY ASSUMPTION, THE MEAN SPEED RATIOS AND MEAN DIRECTION DEVIATIONS (DASHED LINES) ARE OVERPLOTTED. (Data acquired at 150-meter meteorological tower facility at Kennedy Space Center, Florida, from March 16, 1967, to June 12, 1968.)

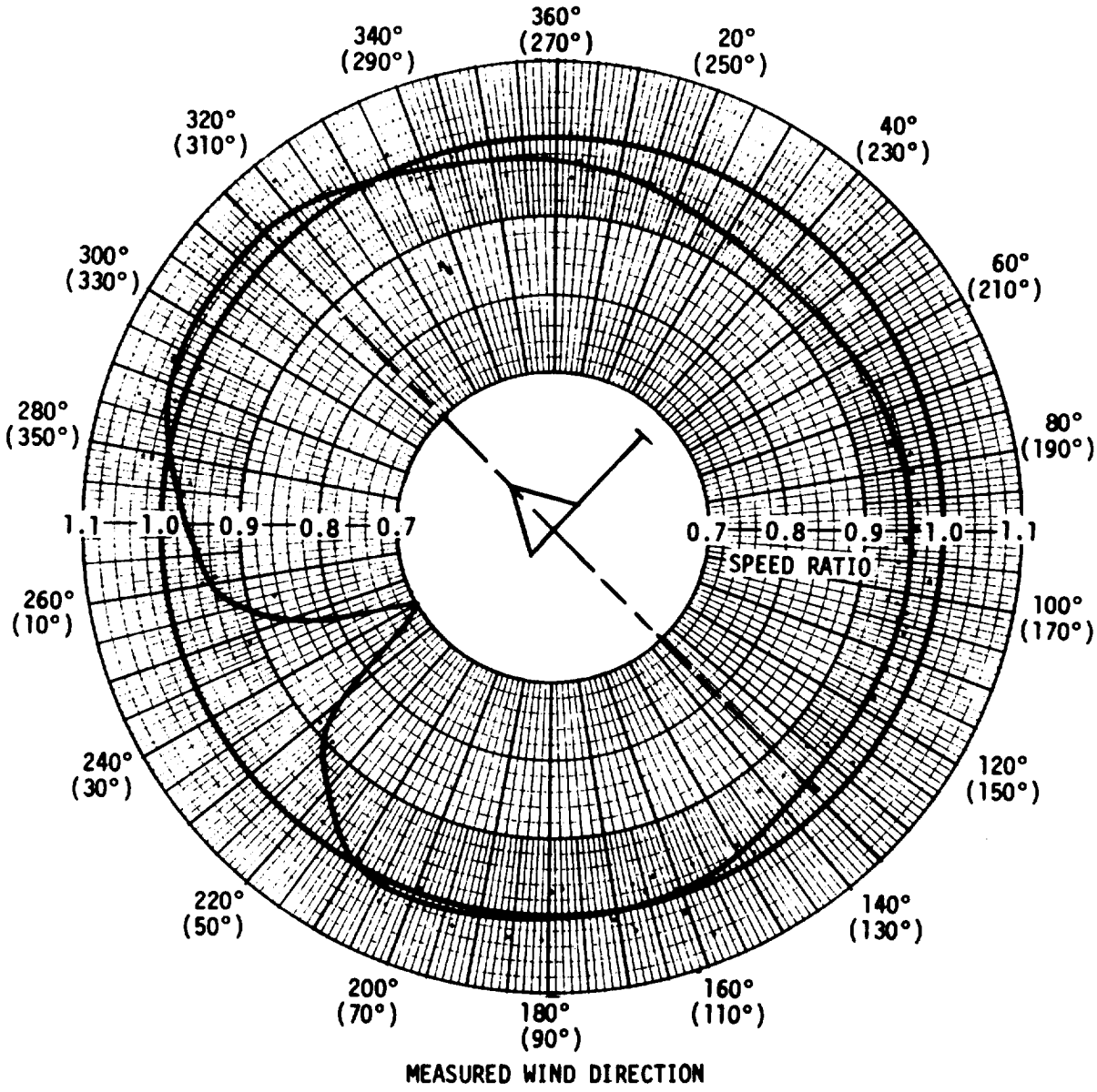

FIGURE 3-9. COMPOSITE INFLUENCE SPEED RATIOS FOR STATIONS 4 AND 5 (DOTS) WITH MEAN INFLUENCE SPEED RATIO (SOLID LINE). (Data acquired at 150-meter meteorological tower facility at Kennedy Space Center, Florida, from March 16, 1967, to June 12, 1968.)

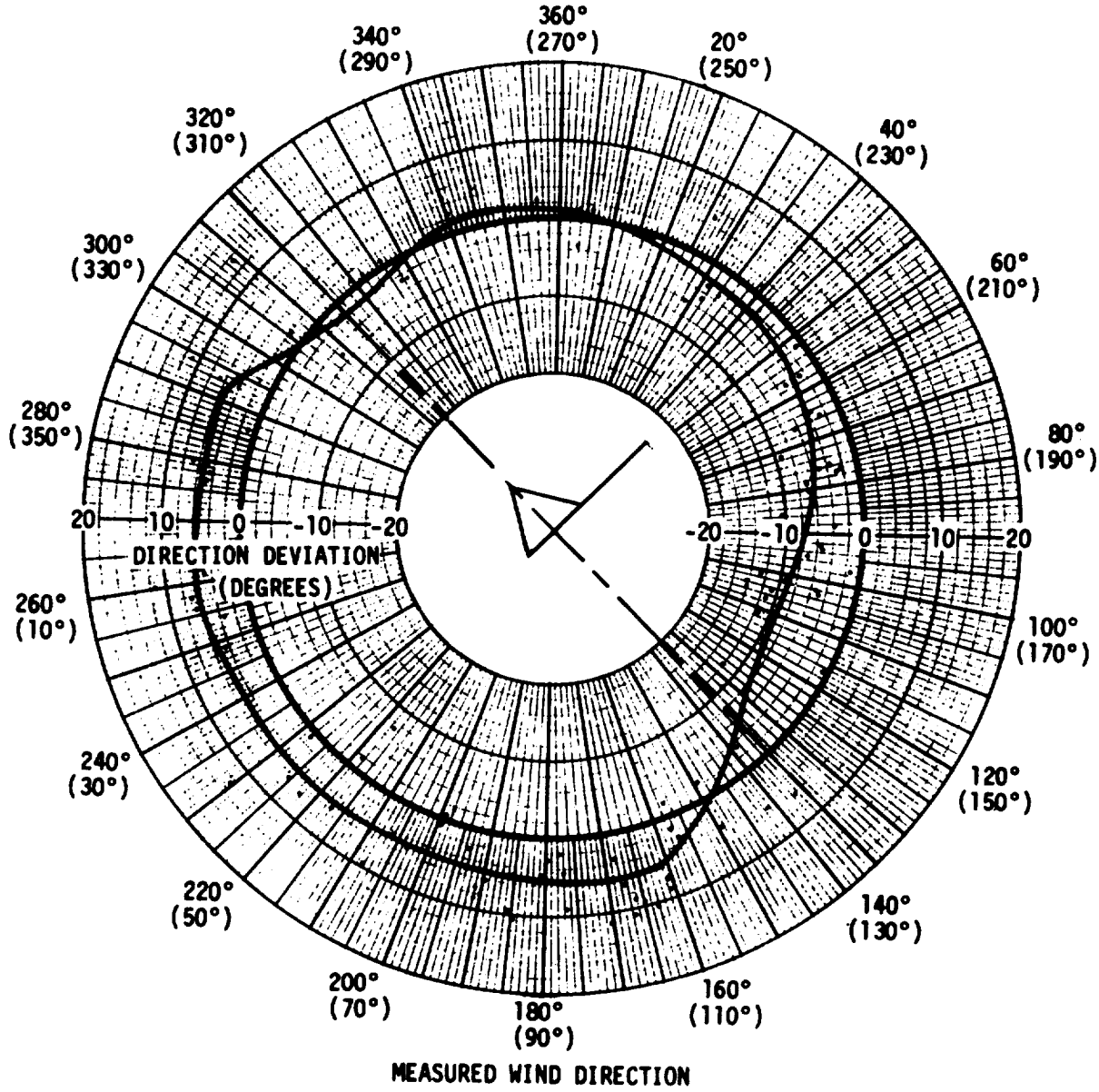

FIGURE 3-10. COMPOSITE INFLUENCE DIRECTION DEVIATIONS FOR STATIONS 4 AND 5 (DOTS) WITH MEAN INFLUENCE DIRECTION DEVIATIONS (SOLID LINE). (Data acquired at 150-meter meteorological tower facility at Kennedy Space Center, Florida, from March 16, 1967, to June 12, 1968.)

3.3.3 (Continued)

if the southwest sensor (Station 4) is the measuring sensor. The solid lines in Figures 3-9 and 3-10 are the mean speed ratios and mean direction deviations that are interpolated from the data points presented in both Figures 3-7 and 3-8.

It can be seen in Figure 3-9 that considerable influence is experienced by the sensor when it is in the lee of the tower (i.e., when the wind is blowing from 240 degrees). The lowest speed ratio calculated is 0.73 (or a 27 percent decrease of the ambient wind speed) for wind direction of 238 degrees; but the lowest interpolated mean ratio is 0.70 at 240 degrees. For winds from the northeast, the speed ratios are generally about 0.96. For winds from the northwest and south-southwest, speed ratios of about 1.02 are measured. The data points plotted on Figure 3-9 provide the user with an estimate of the dispersion encountered in analyzing the data. An attempt to correlate speed ratios and direction deviations to wind speed was unsuccessful. There was insufficient data in the wind speed intervals to draw representative mean values.

It can be seen from Figure 3-10 that the maximum direction deviation occurs at 110 degrees. Dispersion of the data is large in the wake region (around 225 degrees) due to tower-induced turbulence.

Direction sensor calibration is difficult and when comparing sensors, a small error in orienting each sensor can be additive. The dispersion in Figure 3-10 appears considerable; however, the plotting scale and the nature of the data are contributing factors to the data's scattered appearance. By combining direction deviations over the wind speed intervals, valid mean direction deviations were obtained.

To utilize the computed influence factors, mean wind speed and mean wind direction measurements from the northwest sensors on the tower are converted to representative ambient mean wind speed and mean wind direction values in the following manner:

1. Ambient Mean Wind Speed: Take the influence speed ratio from Figure 3-9 at the measured wind direction and divide the measured wind speed by this ratio to obtain the representative ambient mean wind speed.

2. Ambient Mean Wind Direction: Take the influence direction deviation from Figure 3-10 at the measured wind direction and algebraically add this value to the measured mean wind direction to obtain the representative ambient mean wind direction.

If measurements are obtained by one of the southwest sensors, then the measured directions in parentheses on Figure 3-9 and 3-10 should be used. It should be remembered that these influence factors are used as correction factors but are derived from a "reference" sensor in an "undisturbed" location. These correction factors produce wind speed and direction values that are only as representative of the ambient wind as the measurements of

3.3.3 (Continued)

the "reference" sensor. Further, the use of these correction factors to adjust instantaneous speed and direction values is not valid. The correction factors are to be used for 10-minute mean speed and mean direction measurements.

3.4 TOWER INFLUENCE ON TURBULENCE MEASUREMENTS

An unsuccessful attempt was made to determine the tower influence on turbulence measurements using only wind speed data. This influence is the cyclic perturbation to the impinging flow generated by the vortices shedding off of the tower. These cyclic perturbations constitude the wake of the tower and affect the measurement of a sensor in or near the wake.

Since data were acquired simultaneously from both speed sensors at the 30, 90, and 150-meter levels, it was theorized that a comparison of the spectra of a speed sensor in the wake to that of a speed sensor upwind of the tower might give an estimate of the oscillations induced by the tower. This spectra comparison was performed for winds blowing parallel to the boom (from the southwest in Figure 1-2) where a sensor (northeast) would be in the tower's wake. Prior to computing the spectra for winds parallel to the booms, spectra were computed for winds blowing perpendicular to the booms (from the northwest in Figure 1-2) in order to provide an estimate of the "noise" that was obtained when this Power Spectral Density (PSD) computer program operated on wind speed data. These comparisons were made at the 30, 90, and 150-meter levels to check for consistent results at different levels.

Figure 3-11 (a, b, c) presents the PSD's for the set of spectra computed for winds from 328, 322, and 317 degrees (northwest winds) at the 30, 90, and 150-meter levels, respectively. The dispersion between the spectra for the northeast and southwest sensors gives an estimate of the noise to be expected because neither sensor is under any significant tower influence.

Figure 3-12 (a, b, c) presents the PSD's for winds from 224, 215, and 208 degrees for the 30, 90, and 150-meter levels, respectively. Any tower induced variations will appear as an increase or decrease of power for a certain frequency band at the northeast sensor. (For purposes herein, "increases of power" are used as indicators of tower-induced oscillations.) It is also important that this increased power be equivalent in wave length at all levels to insure that the structure of the tower actually does induce these oscillations. Because the structure of the tower is the same at all levels the induced variations should be of approximately the same wave lengths. In Figure 3-12 (a, b, c) increases of power occur at 0.05, 0.06, and 0.08 cycles per second, respectively, that are consistent with 0.06, and 0.08 cycles per second (cps), respectively, that are consistent with the 5.0, 6.3, and 6.5 meters per second measured mean wind speeds that exist at the respective levels (wave length = wind speed/frequency). This, however, would correspond to a period of about 20 seconds which seems too slow an oscillation to represent a tower-induced oscillation. In

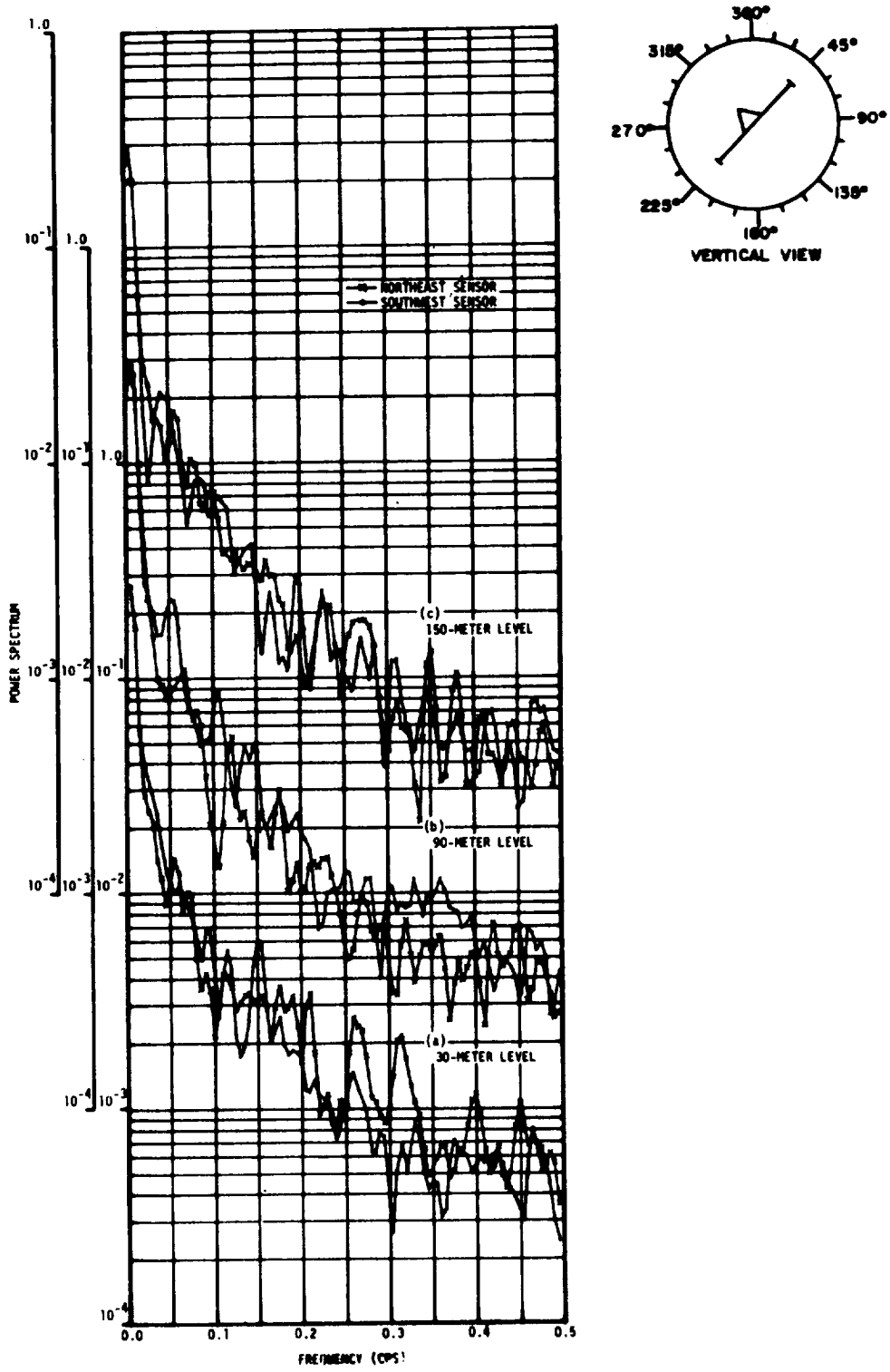

FIGURE 3-11 (a,b,c). POWER SPECTRAL DENSITIES FOR WINDS BLOWING FROM THE NORTHWEST FOR THE 30, 90, AND 150-METER LEVELS. (Data acquired at 150-meter meteorological tower facility at Kennedy Space Center, Florida, from March 16, 1967, to June 12, 1968.)

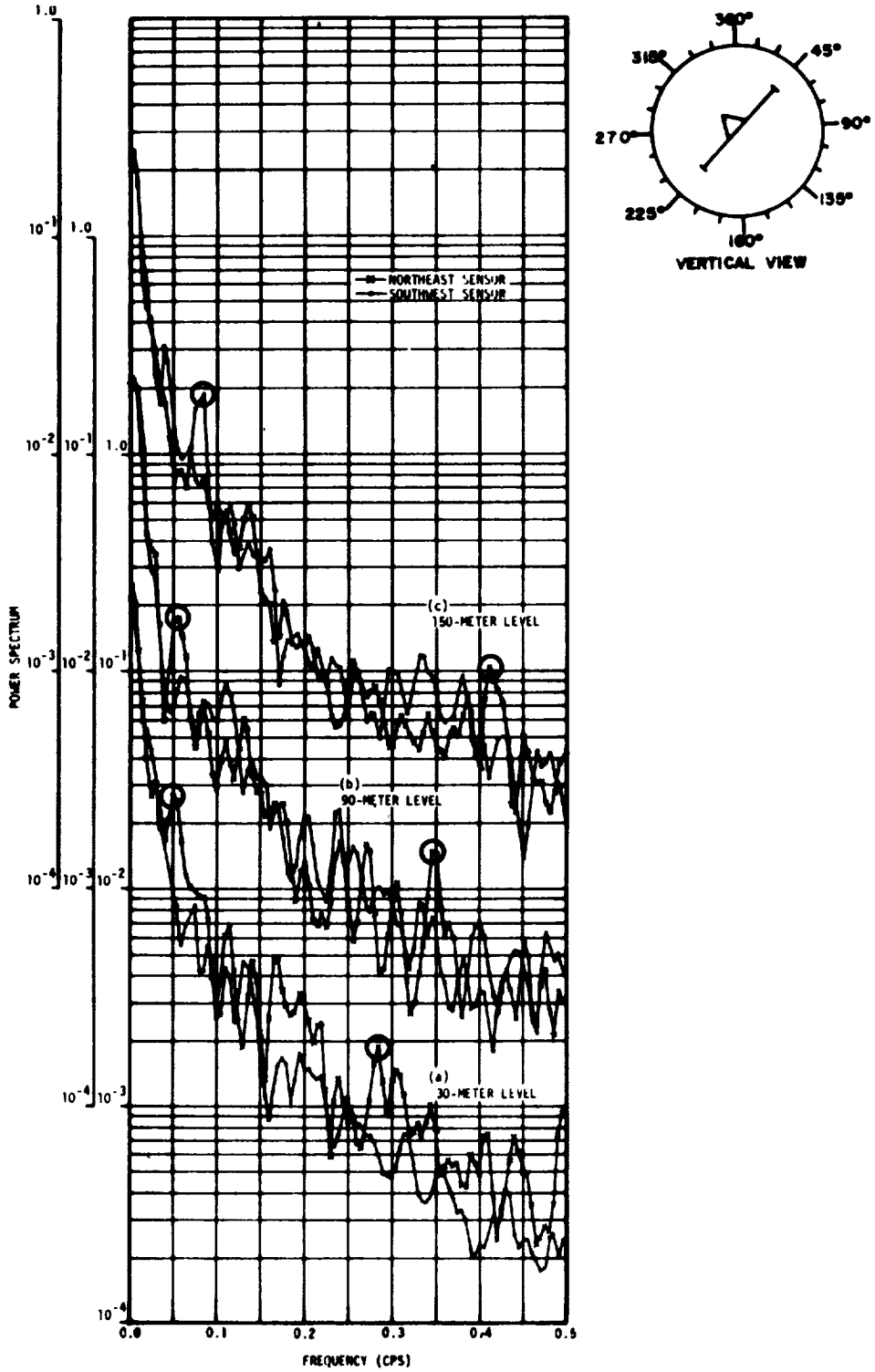

FIGURE 3-12 (a,b,c). POWER SPECTRAL DENSITIES FOR WINDS BLOWING FROM THE SOUTHWEST FOR THE 30, 90, AND 150-METER LEVELS. (Data acquired at 150-meter meteorological tower facility at Kennedy Space Center, Florida, from March 16, 1967, to June 12, 1968.)

3.4 (Continued)

Figure 3-12 (b, c) an increase is noted at 0.35 and 0.41 cps, respectively, that is also consistent with the above measured wind speeds. Projecting these down to the 30-meter level (Figure 3-12 [a]), a consistent increase is noted at 0.285 cps. They are consistent in that the tower would induce an oscillation of about 16 meters wave length or a period of about 3 seconds. One-second data are used in this set of computations, thus limiting the maximum frequency to 0.5 cps. Similar computations were made for this same set of input data taken from the analog tape at a tenth of a second; however, no increases were noted at higher frequencies (0.5 to 5.0 cps) that were consistent enough to be considered significant. The cross-spectra and coherence estimates computed for these cases showed that there were no significant differences between the spectra of either sensor that could be interpreted as a band of frequencies over which the tower was inducing oscillations.

PSD's that were computed for other test cases did not show any increases that were consistent at all levels. It was, therefore, concluded that spectra from wind speed data alone were not sufficient to determine the tower-induced oscillations. It is suggested that atmospheric stability data be incorporated in any additional study because the "base level" ambient wind oscillation in the PSD computations varies considerably and must be taken into consideration.

THIS PAGE INTENTIONALLY LEFT BLANK.

SECTION 4

CONCLUSIONS AND RECOMMENDATIONS

4.0 CONCLUSIONS

From the literature search, it was determined that NASA's 150-meter meteorological tower is of the proper construction and the sensors are oriented to the tower in such a way that the tower poses minimal influence on the upwind sensor. The orientation of the dual booms to the tower (along with the implementation of an automatic direction selector), the location of the sensors at a distance of 1 1/2 D from the corner of the tower, and the lattice type structure of the tower are factors that contribute to the low influence.

It was determined that the assumptions of bilateral symmetry of the field of influence and similarity of the influence field at all levels are, indeed, valid for the prototype tower. Influence factors computed for the 18-meter level can be used at any level of the tower without making corrections for turbulence or atmospheric stability.

The greatest influence the tower induces is in the wake with a speed ratio of 0.70. A general velocity decrease (ratio of 0.94) is noted upwind of the tower and a velocity increase (ratio of 1.02) is noted abreast of the tower outside of the wake. Direction deviations are maximum (-9 degrees) for winds from the east-southeast and are minimum for winds from the north quadrant. The speed ratios computed herein agree fairly well with the ratios computed in the wind tunnel by Vellozzi (Reference 6) using a "clean" scale model of NASA's tower; however, the direction deviations vary for some directions.

The speed ratio computed experimentally for winds from 315 degrees was 1.03 and for winds from 135 degrees was 0.96. These specific wind directions were used in the theoretical cases discussed in Appendix A. A theoretical speed ratio of 1.045 was obtained for the case of a solid tower with catwalk. This case is, theoretically, the maximum influence possible for a triangular tower. The experimentally computed speed ratio of 1.03 for 315 degree winds is less than the theoretically computed maximum of 1.045 and the experimentally computed speed ratio of 0.96 for 135 degree winds is well below the theoretically computed value.

It was determined that the use of wind speed signals is not sufficient as the sole input for the determination of tower-induced oscillations in the wake. A tower-induced oscillation with a wave length of 16 meters (period of 3 seconds) was found to be consistent at all levels for one test case; however, other spectra did not substantiate this or any other wave length oscillation as being significant of the tower's influence.

4.1 RECOMMENDATIONS

The limited data volume did not permit the computation of a set of correction factors, as presented in Figures 3-9 and 3-10, for each of the wind speed ranges of Table 3-I. This occurred because ambient wind variations over a ten-minute time span and the difficulty in calibrating wind direction sensors contribute to the scatter of ratios and deviations that necessitated "mass averaging" to achieve reliable mean values. To completely define the tower influence over the full domain of wind speeds, more data are required. The redefinition of the correction factors for the various speed ranges need only be carried out at the 18-meter level using the small tower as reference and the standard hourly winds obtained over the next few years as input because correction factors computed for the 18-meter level can be applied to the upper levels (see Paragraph 3.3.2).

Since wind speed signals are not sufficient for the determination of tower-induced turbulence, it is recommended that a future wake spectra study be designed to subtract the "base level" of atmospheric turbulence, computed as a function of stability, from the wind speed spectra, then to cross-correlate the leeward and windward sensors to compute cross-spectra and coherence estimates.

The scope of this experiment did not include a study of tower end effects. It is suggested that a study be implemented to determine the existence and define the extent of these effects. The "towing-water tank" technique used by Sanuki and Tsuda (Reference 5) and discussed in Paragraph 2.1.4 could be employed for this definition.

APPENDIX A

A THEORETICAL APPROACH TO THE STUDY OF WIND TOWER INFLUENCE

1.0 POTENTIAL FLOW

The theoretical approach to the tower influence problem assumes that the atmosphere is an ideal fluid (i.e., an inviscid and an incompressible fluid); thereby permitting the use of potential theory in computing the flow about a tower. Two-dimensional flow is also assumed applicable by neglecting the end effects of the tower. These assumptions are considered valid because:

a. Inviscid Fluid: An inviscid fluid is assumed valid because the region of interest is windward of the tower where laminar flow is assumed. Consideration need only be given to the windward side of the tower, since NASA's 150-meter tower has a dual boom arrangement insuring that one sensor will be in the windward half of the compass.

b. Incompressible Fluid: An incompressible fluid is assumed valid because the low free-stream velocities will not produce Mach number (M = speed of ambient wind/speed of sound) conditions greater than 0.2 at any point of interest in the flow field. This low Mach number condition is less than the five percent empirical limit set for incompressible flow as seen by:

$$\frac{\rho_0}{\rho} = (1 + 2M^2)^{2.5} < 1.05$$

where ρ_0 is the ambient density and ρ is density.

c. Two-Dimensional Flow: The end effects of the tower are minimal. Forrest, et al. (Reference 14) imply that the end effects exist for about one to two calibers (where a caliber is a ratio of width of tower to height of influence along tower). Since the tower is eight feet wide, one to two calibers will yield end effect influences of from eight to sixteen feet from the ends of the tower. The 150-meter height of the tower restricts the three-dimensional effects to those portions of the tower near the ground and near the top.

2.0 METHODS OF SOLUTION

The tower influence problem is solvable by utilizing potential theory for determining the flow (i.e., computing the stream function that is the complex conjugate of the velocity potential) if given the boundary conditions associated with the tower. Since the wind sensors are mounted at the boom tips, the influenced flow at these points is required. This flow is easily calculated for a simple geometric figure such as a cylinder; however, difficulties arise in solving the mathematical problem for a tower of lattice structure. The first approximation made to simplify the boundary conditions then

2.0 (CONTINUED)

is to assume that the tower is a solid equilateral triangle. The solid tower represents a larger obstruction to free-stream flow than the lattice tower; therefore, its influence is greater and hence provides an upper bound for the influence of a lattice type tower. A wind tunnel demonstration of this greater influence was performed by Gill, et al. (Reference 2). The directional deviations due to flow about a triangular lattice tower are seen in Figure A-1; those due to flow about a solid triangular tower, are seen in Figure A-2. The solid tower, as expected, causes greater directional deviations upwind than does the lattice tower. Also the solid tower has a larger and more perturbed wake than does the lattice tower. Thus, by computing the flow about a solid triangular tower, the maximum possible influence of any triangular tower, with any degree of porosity, is computed. Because the influence at the boom-tip positions varies with tower orientation to the wind and because the greatest influence occurs when the booms are perpendicular to the free-stream flow, the perpendicular orientation is used in the computation of the maximum influence. It can be seen from Figure A-2 that for this tower orientation to the wind, the tower influence is symmetrical about the centerline of the wind tunnel. To compute the case of maximum tower influence, only half of the tower and its associated flow need be considered (see shaded area of Figure A-3).

The two-dimensional solution for the flow about an object can be obtained analytically using conformal mapping into a complex plane or numerically using digital techniques. A two-dimensional solution for the solid triangle is obtained by numerically solving Laplaces partial differential equation using finite difference methods. To insure that the numerical solutions are reasonable, analytical solutions for two limiting cases (a circular cylinder and a fence) are computed.

2.1 NUMERICAL SOLUTION

2.1.1 Description of Numerical Solution

The numerical solution is obtained using a digital computer program, the Boeing Thermal Analyzer (Reference 15), that employs an over-relaxation technique to solve Laplace's Equation:

$$\nabla^2 \psi = 0 \qquad \text{(A-1)}$$

where ψ represents the stream function.

The Boeing Thermal Analyzer Program solves Equation A-1 for ψ at specified points in a field with the flow assumed horizontal and with a speed of unity. The field is represented by a gridwork of nodes positioned such that they incorporate the geometrical aspects of the problem (represented by the shaded area of Figure A-3) and from which the program derives the finite difference equations for solution. The proper boundary conditions are incorporated by specifying fixed potentials at known streamline positions. For the flow field about the solid triangular tower, the lower and upper boundaries are fixed streamlines. The lower boundary is the axis-of-symmetry

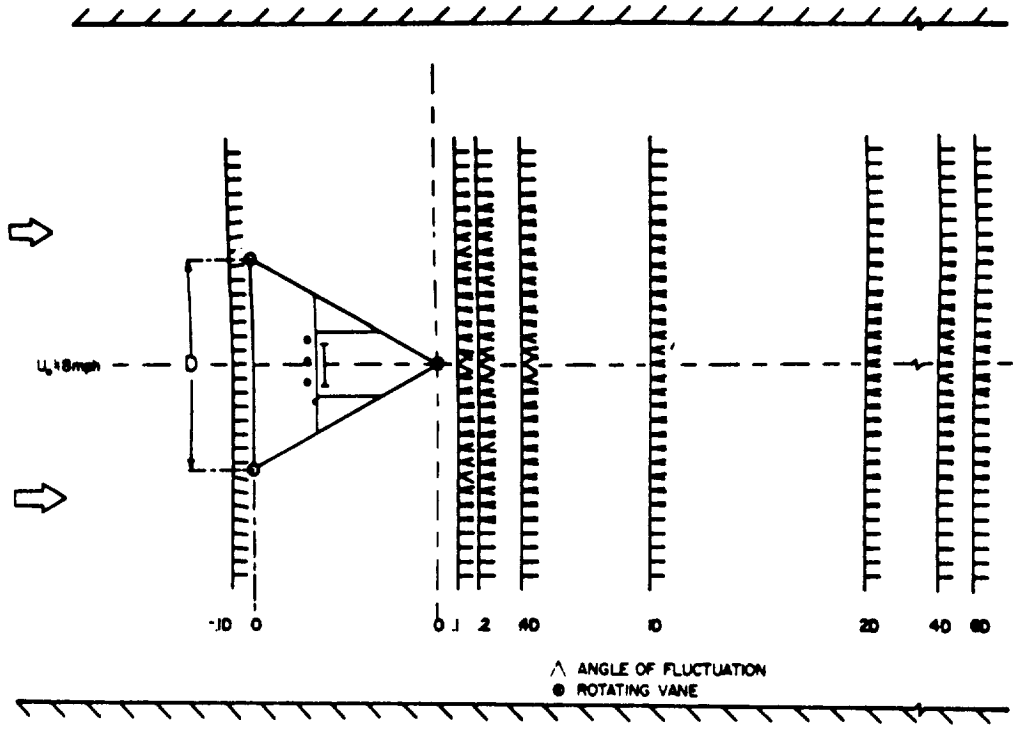

FIGURE A-1. DIRECTIONAL DEVIATIONS ABOUT TRIANGULAR LATTICE TOWER DEMONSTRATING REGIONS OF LAMINAR AND TURBULENT FLOW. (AFTER GILL,OLSSON, AND SUDA - REFERENCE 2).

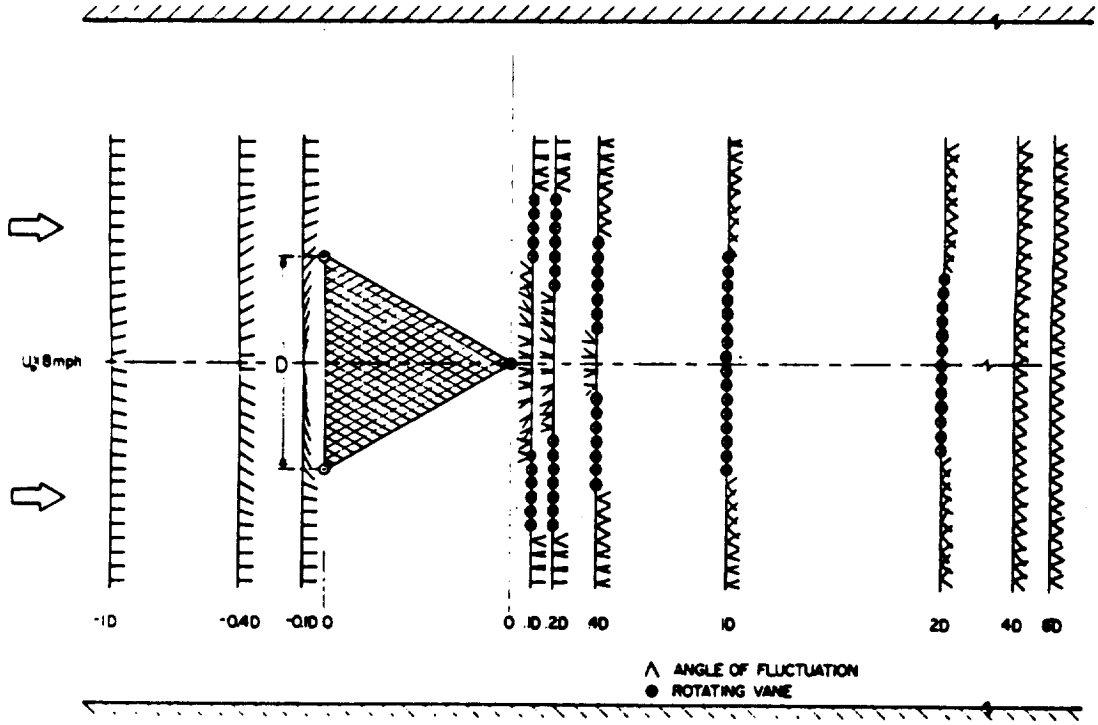

FIGURE A-2. DIRECTIONAL DEVIATIONS ABOUT SOLID TRIANGULAR TOWER DEMONSTRATING REGIONS OF LAMINAR AND TURBULENT FLOW. (AFTER GILL, OLSSON, AND SUDA - REFERENCE 2).

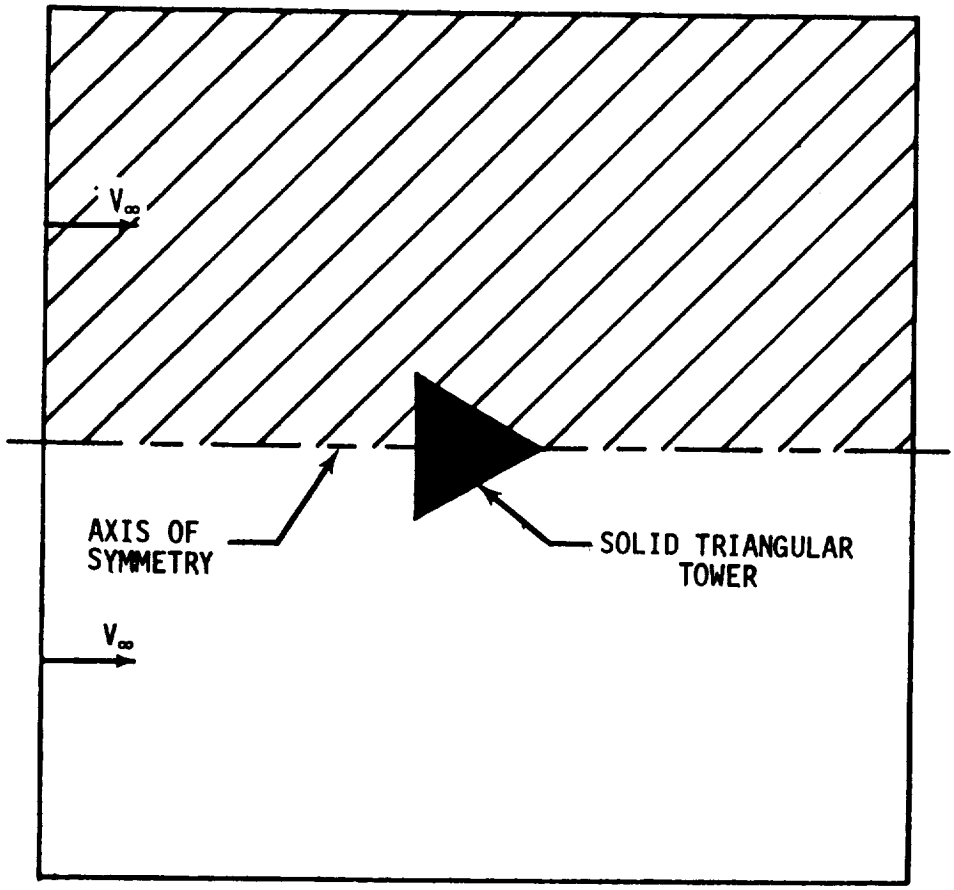

FIGURE A-3. WITH THE AXIS OF SYMMETRY EXISTING THROUGH THE SOLID WIND TOWER, ONLY HALF OF THE FLOW FIELD (SHADED AREA) NEED BE MODELED.

2.1.1 (Continued)

line (CDEFG in Figure A-4) and is specified with a potential of zero. The upper boundary is a straight line (AB) positioned at a distance from the tower where the tower influence is assumed negligible (AC=BG=28 feet) and is specified with a potential such that $\partial\psi/\partial y = V_X = 1$. The left (AC) and right (BG) boundaries are open and located sufficiently far from the tower to represent free-stream conditions.

The relaxation process computes the potential at each node within the field until a steady-state condition exists. The lines of constant potential between the upper and lower boundaries are then established by interpolation and represent the lines of constant stream-function, ψ (or streamlines). The velocity components, V_X and V_Y, at points throughout the field are given by approximating, with appropriate finite difference expressions, the partial derivatives of the stream function in the Y and X directions, respectively, i.e.,

$$V_X = \frac{\partial\psi}{\partial Y} \qquad V_Y = -\frac{\partial\psi}{\partial X}$$

The resultant velocity is given by:

$$V = \sqrt{V_X^2 + V_Y^2}$$

2.1.2 Tower Configurations Used for Numerical Solutions

The solutions for two lower boundary configurations are provided. The first configuration (Figure A-4) models the solid triangular tower from which influences at three sensor locations are determined. Points H and I of Figure A-4 are sensor locations that pertain to winds in the positive X direction (from A to B), and points I and J are sensor locations that pertain to winds in the negative X direction (from B to A).

The second configuration (Figure A-5) models the solid triangular tower with an attached solid rectangle simulating the catwalk. Since the boom is parallel to the catwalk, point I of Figure A-5 is the only sensor location for which wind values are interpretable. It should be noted that this position pertains to winds from either X direction.

2.1.3 Results of Numerical Solution

The flow field about the solid triangular tower and the associated velocity ratios, V/V_∞, are presented in Figure A-6 for winds in the positive X direction and in Figure A-7 for winds in the negative X direction. The velocity ratio at point H in Figure A-6 is 0.980, and the direction deviation is less than three degrees. The velocity ratio at point I in Figure A-6 or A-7 is

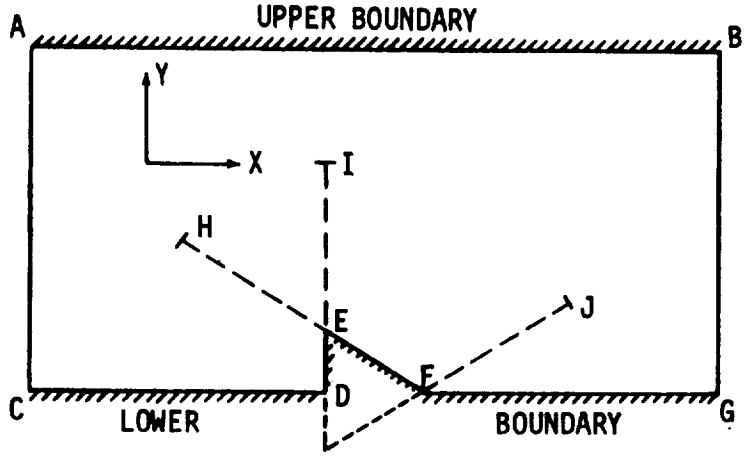

FIGURE A-4. SETUP FOR SOLID TRIANGULAR TOWER - WITH H,I,J, REPRESENTING SENSOR LOCATIONS FOR VARIOUS TOWER ORIENTATIONS

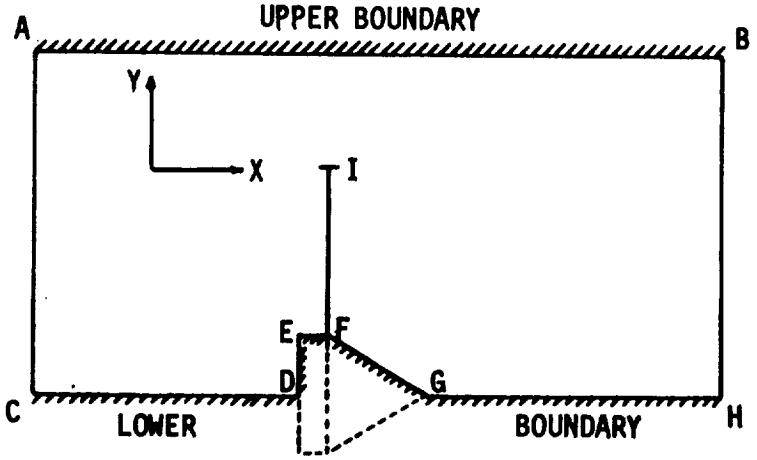

FIGURE A-5. SETUP FOR SOLID TRIANGULAR TOWER WITH SOLID CATWALK - WITH I REPRESENTING THE SENSOR LOCATION AT THE BOOM TIP

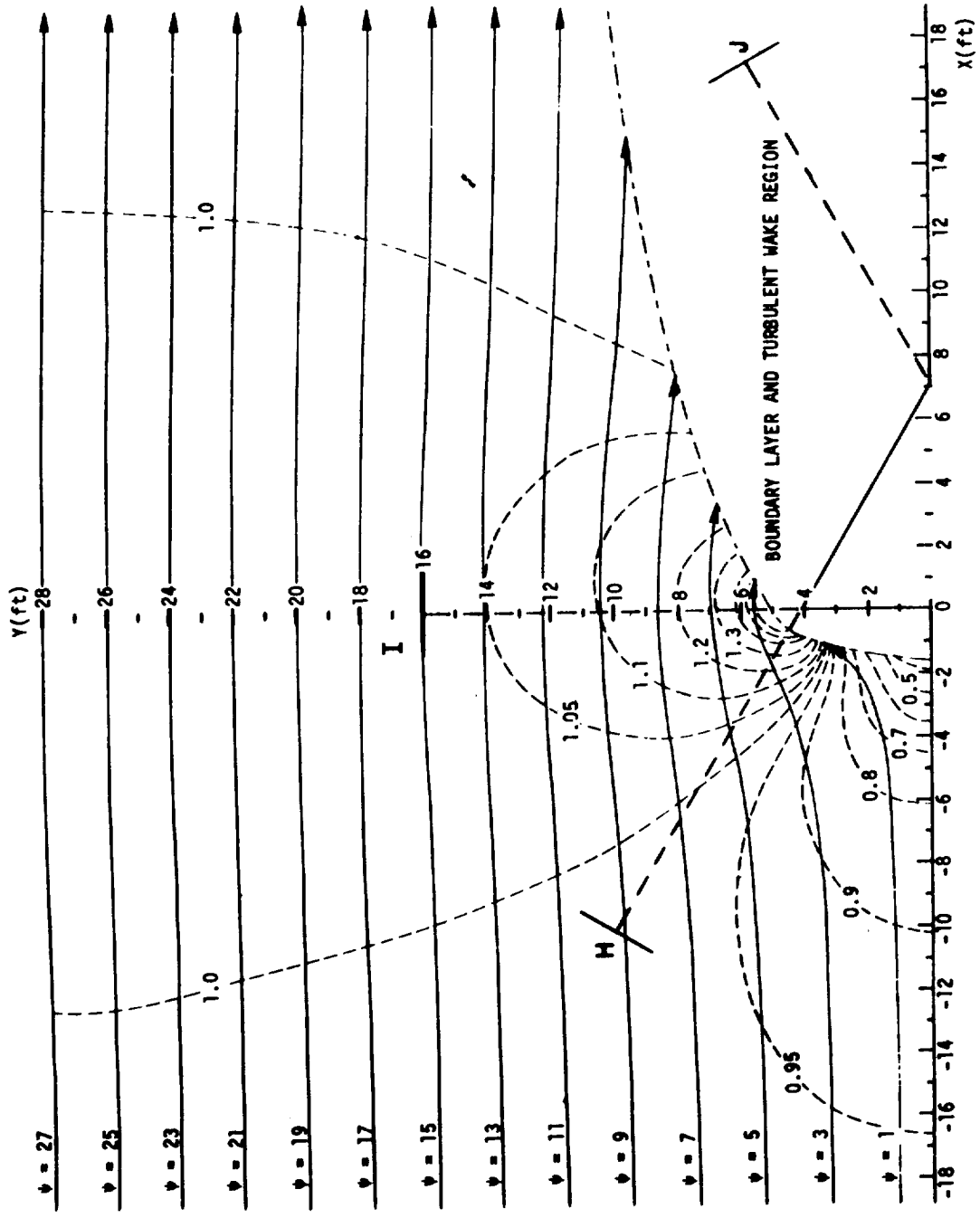

FIGURE A-6. FLOW FIELD (STREAMLINES - SOLID) AND VELOCITY DISTRIBUTION (ISOTACHS - DASHED) ABOUT THE SOLID TRIANGULAR TOWER FOR FLOW TOWARD THE POSITIVE X DIRECTION

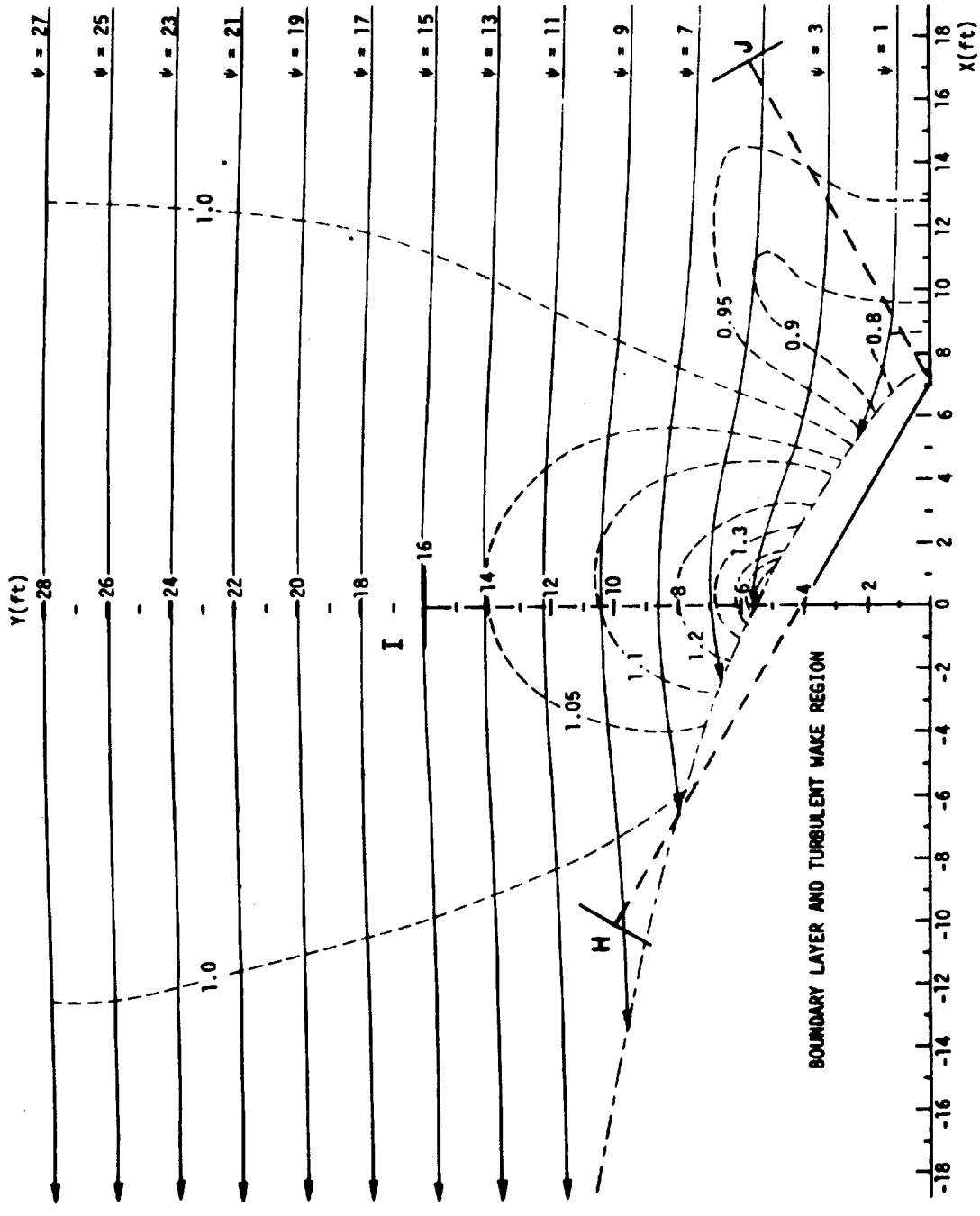

FIGURE A-7. FLOW FIELD (STREAMLINES - SOLID) AND VELOCITY DISTRIBUTION (ISOTACHS - DASHED) ABOUT THE SOLID TRIANGULAR TOWER FOR FLOW TOWARD THE NEGATIVE X DIRECTION

2.1.3 (Continued)

1.035, and the direction deviation is zero degrees. The velocity ratio at point J in Figure A-7 is 0.958, and the direction deviation is less than one degree.

The flow field about the solid triangle with catwalk and the associated velocity ratios are presented in Figure A-8 for winds in the positive X direction and in Figure A-9 for winds in the negative X direction. The velocity ratio at point I is 1.045 and the direction deviation is less than one degree.

The superposition of the boundary flow and turbulent wake regions (taken from Figure A-2) are provided to indicate the regions where interpretation of the wind velocities is not valid.

2.2 ANALYTICAL SOLUTION

Two analytical solutions are included to provide a comparison with the numerical solutions. They are (1) the classical case of flow about a cylinder and (2) the case of flow over a fence of infinitesimal thickness. These cases should provide solutions of both greater and lesser influences, respectively, than those for which numerical solutions are derived (i.e., solid triangle and triangle with catwalk).

The complex potential for the cylinder, $\phi(X + iY)$, is computed in the classical fashion (see Reference 16) by:

$$\phi(Z) = V_\infty \left[X\left(1 + \frac{a^2}{X^2+Y^2}\right) + iY\left(1 - \frac{a^2}{X^2+Y^2}\right)\right]$$

where $Z = (X + iY)$; a is the radius of the cylinder, V_∞ is the free-stream velocity, and X and Y are coordinates. The value of the stream function, ψ, is computed by:

$$\psi = V_\infty Y\left(1 - \frac{a^2}{X^2+Y^2}\right)$$

with a streamline being ψ = constant. The velocity field is computed by:

$$\frac{d\phi}{dZ} = V_\infty\left(1 - \frac{a^2}{Z^2}\right)$$

with the magnitude of the velocity computed by:

$$\left|\frac{d\phi}{dZ}\right| = V_\infty\left(1 - \frac{a^2[2(X^2-Y^2)-a^2]}{(X^2+Y^2)^2}\right)^{\frac{1}{2}}$$

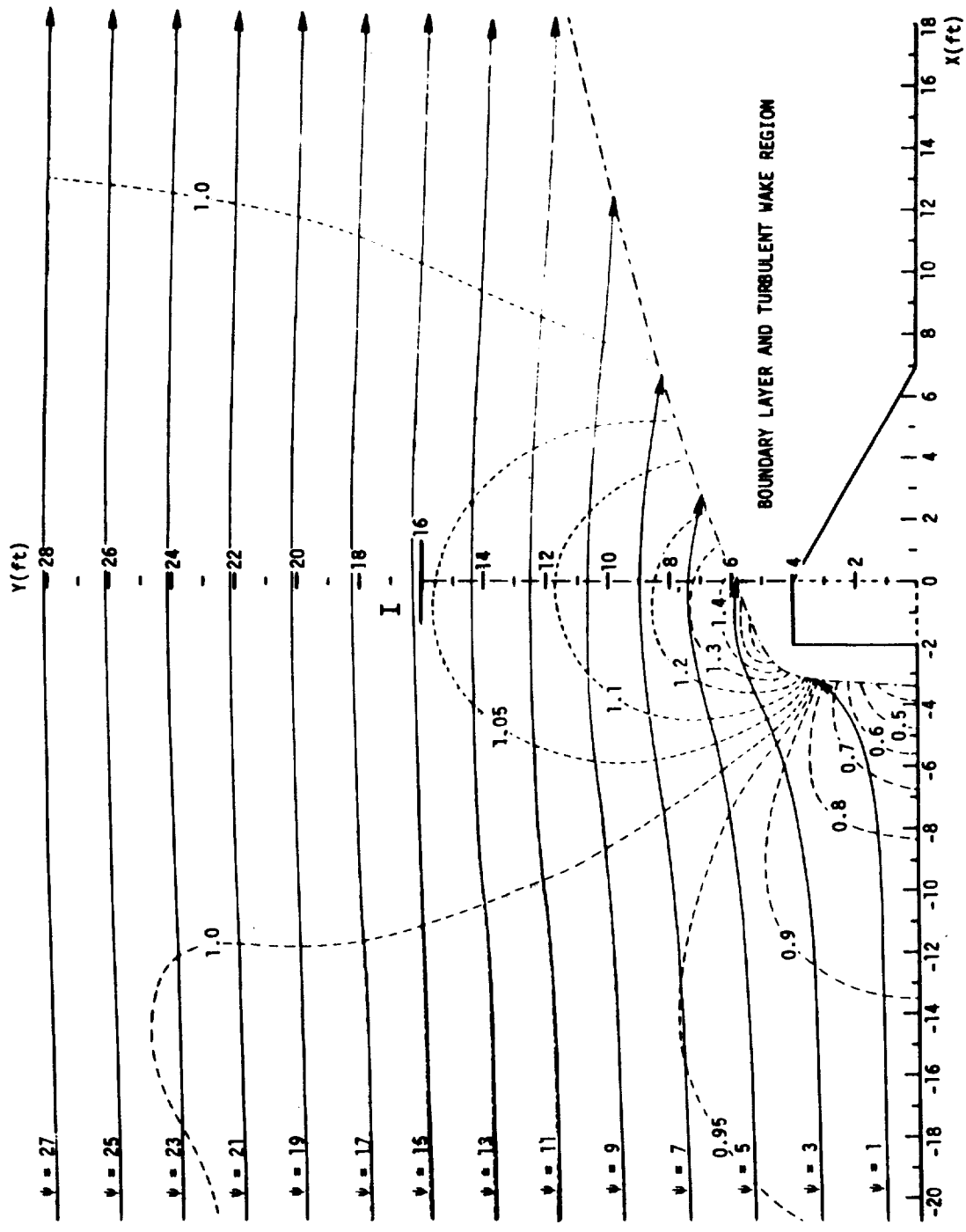

FIGURE A-8. FLOW FIELD (STREAMLINES - SOLID) AND VELOCITY DISTRIBUTION (ISOTACHS - DASHED) ABOUT THE SOLID TRIANGULAR TOWER WITH CATWALK FOR FLOW TOWARD THE POSITIVE X DIRECTION

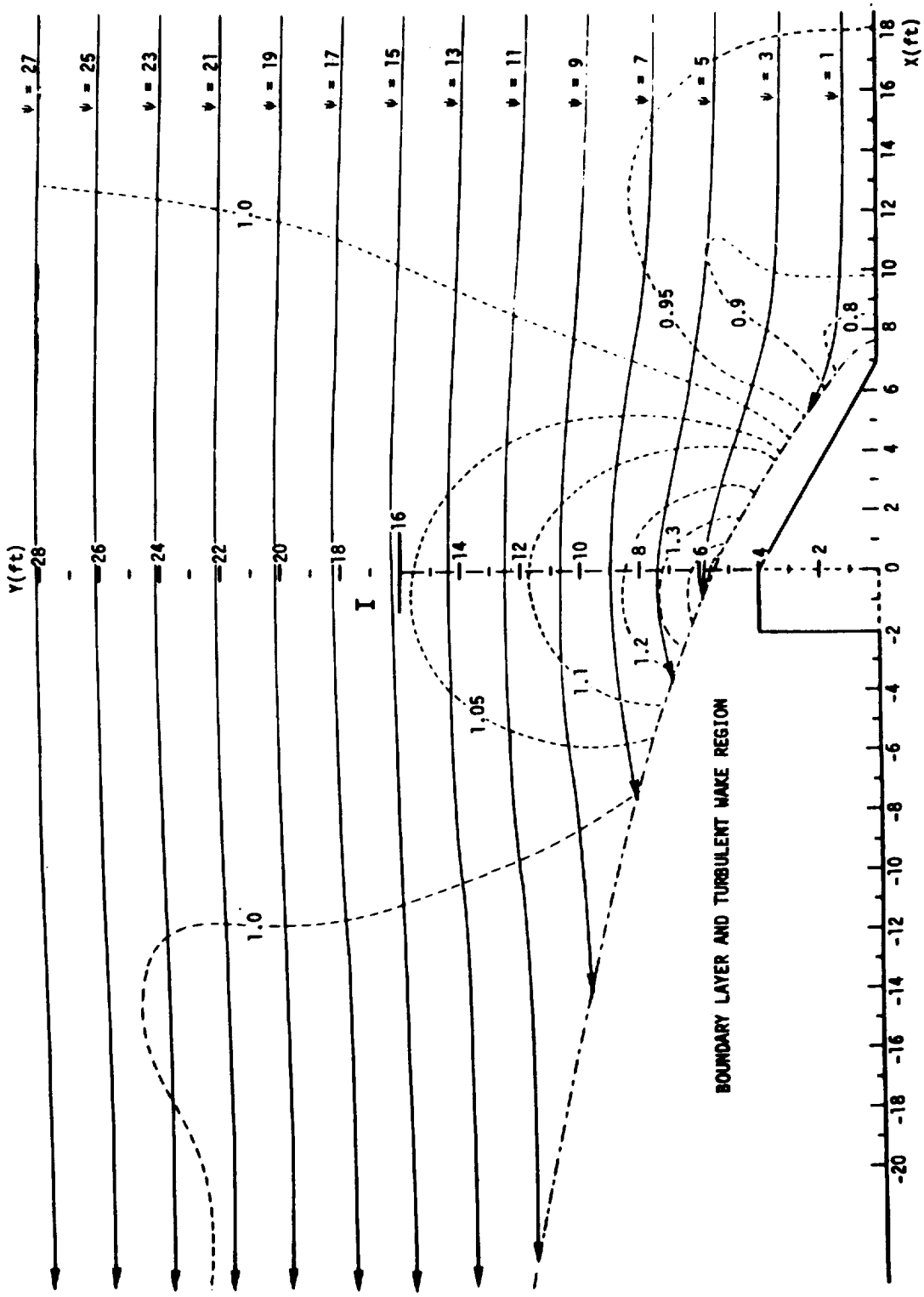

FIGURE A-9. FLOW FIELD (STREAMLINES - SOLID) AND VELOCITY DISTRIBUTION (ISOTACHS - DASHED) ABOUT THE SOLID TRIANGULAR TOWER WITH CATWALK FOR FLOW TOWARD THE NEGATIVE X DIRECTION

2.2 (CONTINUED)

The potential flow over the fence is computed using the Schwartz-Christoffel transformation (Reference 16) in which the complex potential is expressed as:

$$\Phi(Z) = V_\infty[(X+iY)^2 + a^2]^{\frac{1}{2}}$$

where V_∞ is a real constant (free-stream velocity) and "a" is the height of the fence.

Substituting $\Phi = (\phi + i\psi)$ for the velocity potential, then

$$(\phi + i\psi)^2 = V_\infty^2 [(X + iY)^2 + a^2]$$

$$\phi^2 - \psi^2 = V_\infty^2 (X^2 - Y^2 + a^2)$$

$$\phi\psi = V_\infty^2 XY$$

The stream function is computed by:

$$\frac{V_\infty^4 X^2Y^2}{\psi^2} - \psi^2 = V_\infty^2 (X^2 - Y^2 + a^2)$$

and the velocity field is computed by:

$$\frac{d\Phi}{dZ} = V_\infty \left(\frac{X^2 - Y^2 + i2XY}{X^2 - Y^2 + a^2 + i2Y} \right)^{\frac{1}{2}}$$

with its magnitude computed by:

$$\left|\frac{d\Phi}{dZ}\right| = V_\infty \left[\frac{(X^4 + 2X^2Y^2 + a^2X^2 - a^2Y^2 + Y^4)^2 + 4a^2X^2Y^2}{(X^4 + 2X^2Y^2 + 2a^2X^2 + Y^2 - 2a^2Y^2 + a^4)^2} \right]^{\frac{1}{4}}$$

The solution of greater influence is provided by the flow about the solid cylinder. At the boom-tip position (X = 0, Y = 16 feet), the velocity ratio is 106.25 for the solid cylinder (Figure A-10) and 103.28 for the solid fence (Figure A-11). These demonstrate that the numerical solutions for the solid triangle with and without catwalks are reasonable and fall within the computed limiting cases.

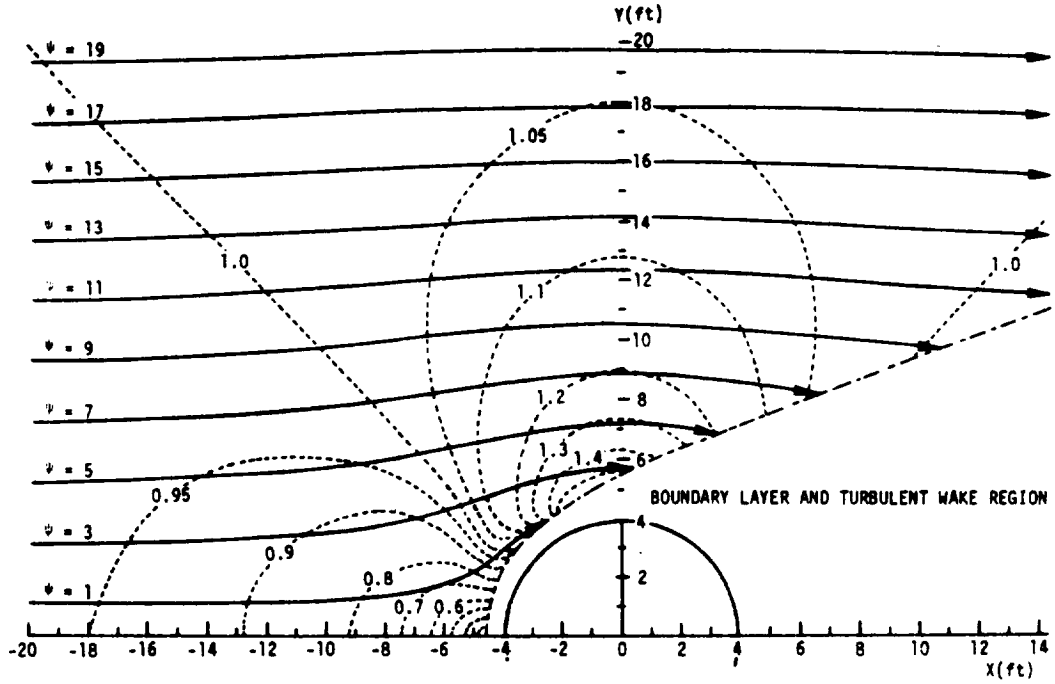

FIGURE A-10. FLOW FIELD (STREAMLINES - SOLID) AND VELOCITY DISTRIBUTION (ISOTACHS - DASHED) ABOUT THE SOLID CYLINDER

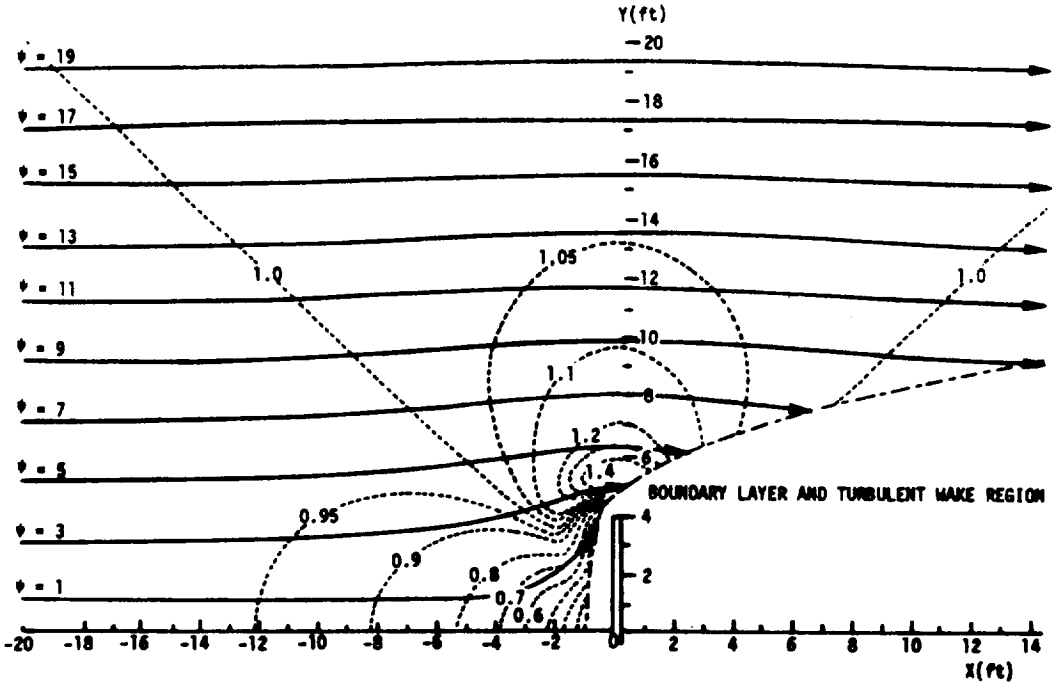

FIGURE A-11. FLOW FIELD (STREAMLINES - SOLID) AND VELOCITY DISTRIBUTION (ISOTACHS - DASHED) ABOUT THE SOLID FENCE

3.0 CONCLUSIONS

Any obstruction to the flow that is posed by the turbulent region is not modeled. For the modeled solid towers (with and without catwalks), the influence at the boom-tip positions (boom length = $1\frac{1}{2}$ times the width of the tower) of the anemometers is always less than five percent in wind speed and less than three degrees in wind direction. These values correspond well to those computed analytically for the cylindrical case where a maximum of six percent increase in wind speed is determined for the same anemometer position. As demonstrated in a referenced report (Reference 2), perforating the tower structure permits an easing of the amounts of influence at the boom-tip positions. No solution for a perforated tower is presented, but this decrease of the tower influence suggests that the five percent influence is the maximum for any triangular tower.

In the instance when the boom-tip position of the sensor is between 120 and 150 degrees from the direction of the wind, velocity ratios of 1.01 to 1.10 are recorded experimentally (see Table 2-I). Modeling, performed herein, does not consider influences in the turbulent wake so no comparison with these experimental results can be made. Fortunately, NASA's 150-meter meteorological tower has sensors on either side of the tower such that the sensor in the wake position need not be monitored.

DISTRIBUTION

DEP-T

R-EO
Dr. Johnson

R-SE
Mr. Belew (2)
Mr. E. May

R-SSL
Dr. Stuhlinger

R-COMP
Dr. Hoelzer
Mr. R. Cochran
Mr. P. Harness

R-P&VE
Dr. Lucas
Mr. R. Goerner
Mr. Kroll (2)
Mr. Hunt
Mr. Showers
Mr. Moore
Mr. Stevens

R-ASTR
Dr. Haeussermann
Mr. Blackstone
Mr. Mink
Mr. Hosenthien

I-MT
Mr. Lee Nybo

I-MO
Dr. F. Speer

I-V
Mr. L. James

I-I/B
Col. W. Tier

MS-IP

MS-IL (8)

MS-H

HME-P

PAT

MS-T (6)

I-RM-M

R-AERO
Dr. Geissler
Mr. Jean
Mr. Thomae
Mr. Dahm
Mr. Holderer
Mr. Reed
Mr. Horn
Mr. R. Walker
Mr. Verderaime
Mr. Rheinfurth
Mr. Ryan
Mr. Lindberg
Mr. Stone
Mr. Hagood
Mr. T. Deaton
Mr. Hardage
Mr. G. Weisler
Mr. Baker
Mr. Thionnet
Mr. R. Lavender
Dr. Heybey
Mr. J. Kaufman (50)
Mr. Fichtl
Mr. Camp
Mr. Hill
Mr. Susko
Mrs. Alexander
Mr. R. Turner
Mr. O. Smith
Mr. C. Brown
Mr. Daniels
Mr. R. Smith
Mr. W. Vaughan (3)
Dr. L. DeVries

NASA Headquarters
Washington, D. C. 20546

Office of Advanced Research and Tech.
ATTN: Mr. Charak
Mr. T. Cooney
Mr. M. Ames
Mr. F. Stephenson
Mr. D. Gilstad
Mr. W. McGowan
Mr. D. Michel (2)

NASA Headquarters (Cont'd)

Office of Space Science & Appli.
ATTN: Dr. W. Tepper
Mr. W. Spreen

NASA-Kennedy Space Center
Kennedy Space Center, Fla. 32899
ATTN: Dr. H. F. Gruene, LV
Dr. Bruns, IN-DAT
Col. Petrone, DE
Mr. Taiani,.AP-OPN-4
Mr. E. Mathews, AP-SAT
Mr. Lester Keene, IN-DAT-2 (10)
Mr. J. Deese, DE-FAC
Mr. R. Clark, TS
Mr. E. Amman, TS-MET
Dr. Knothe, EX-SCI
Mr. Sendler, IN
Mr. P. Claybourne, DE-FSO
Mr. J. Stephens, IN-MSD
Mr. R. Jones, IN-MSD-3

NASA-Langley Research Center
Langley Field, Va. 23365
ATTN: Mr. H. Morgan
Mr. V. Alley
Mr. I. E. Garrick
Mr. W. H. Reed, III (2)
Mr. H. B. Tolefson
Mr. R. Henry
Tech Library (2)

NASA-Lewis Research Center
2100 Brookpark Rd.
Cleveland, Ohio 44135
ATTN: Mr. J. C. Estes
Library (2)

NASA-Manned Spacecraft Center
Houston, Texas 77001
ATTN: Mr. William, PD-5
Mr. D. C. Wade
Mr. John Mayer
Mr. Maynard, PD
Tech Library (2)

Environmental Science Service Admin.
Weather Bureau
Washington, D. C. 20235

Commander
Headquarters, Air Weather Service
Scott AFB, Ill. 62225
ATTN: Dr. R. D. Fletcher
Technical Library (3)

Office of Staff Meteorologist
AFSC (SCWTS)
Andrews AFB
Washington, D. C. 20331

Air Force Systems Command (2)
Space Systems Division
Air Force Unit Post Office
Los Angeles, Calif. 90045

Meteorological & Geoastrophysical
Abstracts
P. O. Box 1736
Washington, D. C. 20013

Air Force Cambridge Research Labs.
Bedford, Mass. 01730
ATTN: Mr. N. Sissenwine
Mr. R. Leviton
Tech Library (3)

Dr. O. Essenwanger
AMSMI-RRA, Bldg. 5429
U. S. Army Missile Command
Redstone Arsenal, Ala. 35809

Mr. Orville Daniel
PAWA/GMRD, AFMTC
MU-235, Technical Library
Patrick AFB, Fla. 32925

Mr. John F. Spurling
NASA, Wallops Island, Va. 23337

Martin-Marietta Corp.
Aerospace Div.
P. O. Box 179
Denver, Colorado 80201
ATTN: Mr. J. M. Bidwell

Air Force Flight Dynamics Lab.
Air Force Systems Command
Wright-Patterson AFB, Ohio 45433
ATTN: Mr. N. Loving (FDTR)

DISTRIBUTION (CONT'D)

Mr. C. D. Martin
Technical Staff
North American Rockwell Corp.
12214 Lakewood Boulevard
Downey, Calif. 90241

Dr. C. E. Buell
Kaman Nuclear
Garden of the Gods Road
Colorado Springs, Colorado. 80907

Dr. Arnold Court
17168 Septo St.
Northridge, Calif. 91324

Space Technology Lab., Inc.
Structures Department
One Space Park
Redondo Beach, Calif. 90277
ATTN: Mr. Marvin White
Mr. Sol Lutwak

Mr. Brian O. Montgomery
MSFC Resident Representative
Kennedy Space Center, Fla. 32899

NASA-Flight Research Center
Edwards AFB, Calif. 93523
ATTN: Mr. J. Ehernberger

Mr. Fred Martin
General Dynamics
5873 Kearny Villa Rd.
San Diego, Calif. 92123

Lockheed Co.
Sunnyvale, Calif. 94088
ATTN: Dr. Geo Boccius
Mr. H. R. Allison

National Center for Atmospheric Rsch.
Boulder, Colorado 80302

Institute for Environmental Research
ESSA - Research Laboratories
Boulder, Colorado 80302

Dr. Hans Panofsky
The Pennsylvania State Univ.
503 Deitu Bldg.
Dept. of Meteorology
University Park, Pa. 16802

Dr. George McVehil
Cornell Aeronautical Lab., Inc.
4455 Genesea St.
Buffalo, New York 14221

Dr. James R. Scoggins
The Texas A&M University
Dept. of Meteorology
College Station, Texas 77843

R. A. Taft Sanitary Eng. Center
Public Health Service
4676 Columbia Parkway
Cincinnati, Ohio 45202

Atmospheric Sciences Lab. (2)
U. S. Army Electronics Command
WSMR, New Mexico 88002

B. N. Charles
Aerospace Corp.
Box 95085
Los Agneles, Calif. 90045

Dr. H. Crutcher (2)
ESSA-NWRC
Asheville, N. C. 28801

Dr. Frank Gifford
Director, Atmospheric Diffusion
Laboratory
U. S. Weather Bureau, ESSA
Oakridge, Tenn. 28111

NASA-Manned Spacecraft Center
WSMR Operations
Post Office Box MM
Las Cruces, New Mexico 88001
ATTN: Mr. A. S. Paczynski
Mr. George Ortiz

DISTRIBUTION (CONT'D)

Mr. C. W. Hines (2)
NASA-Pacific Launch Office
P. O. Box 425
Lompoc, Calif. 93428

Mr. Gene E. Godwin (2)
Programs and Liaison Branch
NASA-Wallops Station, Va. 23337

Mr. Manuel Armendariz
U. S. Army Electronics Rsch &
Devel. Activity
White Sands Missile Range
Las Cruces, New Mexico 88001

Mr. L. J. Rider
Atmospheric Sciences Labs.
U. S. Army Electronics Command
White Sands Missile Range
Las Cruces, New Mexico 88001

Mr. R. K. Jenkins
SELWS-ER
U. S. Army Electronic Rsch. &
Devel. Activity
White Sands Missile Range
Las Cruces, New Mexico 88001

Mr. T. R. Carr
Code 3251, Box 22
Pacific Missile Range
Point Mugu, California 93041

Office of Staff Meteorologist
Air Force Eastern Test Range
Patrick AFB, Fla. 32925

Mr. N. J. Asbridge
WTWU
Air Force Western Test Range
Vandenberg AFB, Calif. 93437

Mr. W. L. Webb
SELWS-E
U. S. Army Elect. Rsch. & Devel. Act.
WSMR, New Mexico 88002

Maj. W. D. Kleis, USAF
SCWT
Air Force Systems Command
Andrews AFB, Md. 20331

LCOL F. J. Franz, USAF
BSOW
Ballistics Systems Division
Norton AFB, Calif. 92409

Mr. V. S. Hardin
AWSAE
Air Weather Service
Scott AFB, Ill. 62226

Mr. K. M. Nagler
Chief, Space Operations Support Div.
U. S. Weather Bureau, ESSA
Silver Springs, Md. 20910

Mr. C. A. Olson
Code 7261
Sandia Corp. Sandia Base
Albuquerque, New Mexico 87110

Mr. Lee L. Sims
USAERDAA, Meteorology Dept.
U. S. Army Electronics Proving Gd.
Ft. Huachuca, Arizona 85613

Mr. Ray E. Bieber
55-76, 102
Lockheed Missile and Space Co.
P. O. Box 504
Sunnyvale, Calif. 94088

Mr. Arthur Belmont
Control Data Dorp.
Minneapolis, Minn. 55440

Mr. Stan Adelfang
Lockheed California Co.
Burbank, Calif. 91500

Mr. Frank Caplan
GCA Technology Div.
A Div. of GCA Corp.
Bedford, Mass. 01730

DISTRIBUTION (CONT'D)

Lockheed Missiles & Space Co.
Huntsville Research & Eng. Cntr.
Orgn 54/50, FAC. 4
P. O. Box 1103-West Station
Huntsville, Ala. 35807
ATTN: Dr. Bowman
Mr. R. DeMandel
Mr. S. Krivo

Dr. Robert Stengel
Dept. of Meteorology
Mass. Institute of Tech.
Cambridge, Mass. 02139

Aerophysics Laboratory
Stanford Research Institute
Menlo Park, Calif. 94025
ATTN: Mr. R. T. H. Collis
Mr. R. M. Endlich

Mr. N. A. Engler
University of Dayton
Dayton, Ohio 45409

LCOL R. F. Durbin, USAF
WTW
Air Force Western Test Range
Vandenberg AFB, Calif. 93437

Mr. Q. S. Dalton
Code 3069
Naval Ordnance Test Station
China Lake, Calif. 93555

Mr. A. J. Krueger
Code 50
Naval Ordnance Test Station
China Lake, Calif. 93555

LCOL B. F. Walker, USAFPGLW
Air Proving Ground Center
Eglin AFB, Fla. 32542

Cdr. W. S. Houston, Jr., USN
Chief, Environmental Science Div.
Office of Asst. Dir.(Rsch)
OSD/Dept. of Defense Rsch. & Engr.
Room 3E-1037, Pentagon
Washington, D. C. 20301

Mr. R. E. McGavin, 520.80
Tropospheric Telecommunications Lab.
Inst. for Telecom Sciences & Aeronomy
ESSA
Boulder, Colorado 80302

Mr. C. J. Callahan
FC-3
Deputy, Fedl. Coordinator for Met.
Services & Supporting Rsch.
U. S. Department of Commerce
ESSA
Washington, D. C. 20235

Maj. R. I. Vick, USAF
PGGW
Air Proving Ground Center
Eglin AFB, Fla. 32542

LCOL I. A. Van Brunt, USAF
WEA
Air Force Flight Test Center
Edwards AFB, Calif. 93523

SSOTW
Air Force Satellite Control Facility
Sunnyvale, Calif. 94086

SSSW
Hq., Space Systems Division
Los Angeles AF Station
Los Angeles, Calif. 90045

Mr. K. C. Steelman
AMSEL-RD-SM
U. S. Army Elect. Rsch. & Deve. Lab.
Ft. Monmouth, New Jersey 07703

Mr. H. D. Bagley
AMSMI-RRA, Bldg. 5429
Physical Science Lab.
Redstone Arsenal, Ala. 35809

Mr. A. L. Miller
AIR-5403
Naval Air Systems Command
Washington, D. C. 20360

DISTRIBUTION (CONT'D)

Mr. R. M. Fenn
KXR, DOD Code 1232
U. S. Naval Weapons Laboratory
Dahlgreen, Virginia 22448

Mr. H. Demboski
Code 421
Office of Naval Research
Washington, D. C. 20360

Cdr. T. H. R. O'Neill, USN
Naval Weather Station
Code 70
Washington (Navy Yard Annex)
Washington, D. C. 20490

Meteorological Division
U. S. Army Signal Research &
Devel. Laboratories
Ft. Monmouth, New Jersey 07703

Meteorology Research, Inc.
464 W. Woodbury Rd.
Altadena, Calif. 91001
ATTN: Dr. P. MacCready
Mr. Brand Nieman

Dr. Thomas A. Gleeson
Florida State University
Department of Meterology
Tallahassee, Florida 32306

Launch System Division
Post Flight Trajectories
The Boeing Company
Mail Stop AD-62
Huntsville, Ala. 35801
ATTN: Mr. R. McCurdy
Mr. J. Hathorn
Mr. R. Wheeler

Mr. Joseph Goldman
Institute for Storm Research
3812 Montrose Boulevard
Houston, Texas 77006

Mr. David Hargis
Solid Mechanics Department
Aerospace Corporation
Bldg. A2, Mail Station 2243
P. O. Box 95805
Los Angeles, Calif. 90045

Mr. George Muller (FDTR)
Air Force Flight Dynamics Lab.
Air Force Systems Command
Wright-Patterson AFB, Ohio 45433

Midwest Research Institute
425 Volker Boulevard
Kansas City, Missouri 64110

Mr. D. T. Penland
Code: TS-TSM-B2
Chief, Apollo/Saturn Project Off.
Kennedy Space Center, NASA
Kennedy Space Center, Fla. 32899

Prof. Elmer R. Reiter
Dept. of Atmospheric Science
Colorado State University
Ft. Collins, Colorado 80521

Mr. Robert M. Slavin
Code: CRE
Air Force Cambridge Research Labs.
(OAR)
Laurence G. Hanscom Field
Bedford, Mass. 01731

Dr. Sidney Teweles (W14)
Chief, Data Acquisition Div.
ESSA, Weather Bureau
8060 13th Street
Silver Springs, Md. 20910

Dr. Yih-Ho Pao
Boeing Scientific Research Lab.
P. O. Box 3981
Seattle, Washington 98124

Dr. H. B. Cramer
GCA Corporation
GCA Technology Division
Bedford, Mass. 01730

Mr. Oscar Lappe
Dept. of Met. & Oceanography
Geophysical Sciences Laboratory
New York University
Bronx, New York 10468

Mr. Ralph Reynolds
Atmospheric Sciences Laboratory
U. S. Army Electronics Command
White Sands Missile Range
Las Cruces, New Mexico 88001

DISTRIBUTION (CONT'D)

Mr. G. C. Gill
University of Michigan
Ann Arbor, Michigan 48104

Mr. J. Vellozzi
Ammann and Whitney
111 Eighth Avenue
New York, New York 10011

Brookhaven National Laboratory
Associated Universities
Upton, L. I. N.Y. 11973
ATTN: Miss Constance M. Nagle
Meteorology Group

Central Electricity Research Laboratories
Cleeve Road
Leatherhead, Surrey
Great Britain
ATTN: John Armitt

Mr. J. E. Cermak
Colorado State University
Boulder, Colorado 80302

Mr. H. Moses
Argonne National Laboratory
Radiological Physical Division
Argmne, Illinois 60439

Dames & Moore
1314 W. Peachtree St., NW
Atlanta, Georgia 30309
ATTN: Frank Courtney

GCA Technology Division
Burlington Road
Bedford, Massachusetts 01730
ATTN: Paul Morgenstern

Scientific and Technical Inf.
Facility (25)
P. O. Box 33
College Park, Md. 20740